T.R.
BOLU ABANT İZZET BAYSAL UNIVERSITY
INSTITUTE OF GRADUATE STUDIES
Department of Physics

SUPERCONDUCTING JOINT STUDIES OF IRON SHEATHED MgB_2 ROUND WIRES BY INDUCTION HEATING METHOD

MASTER OF SCIENCE

BAYRAM ALBAYRAK

ACADEMIC SUPERVISOR
Prof. Dr. Mustafa AKDOĞAN

BOLU, OCTOBER 2024

APPROVAL OF THE THESIS

"Superconducting joint studies of iron sheathed MgB_2 round wires by induction heating method." submitted by **Bayram ALBAYRAK** and defended before the Examining Committe Members listed below in partial fulfillment of the requirements for the degree of **Master of Science** in **Department of Physics, Institute of Graduate Studies of Bolu Abant Izzet Baysal University in 21.10.2024 by**

Jury Members	**Signature**
Supervisor Prof. Dr. Mustafa AKDOĞAN Bolu Abant İzzet Baysal University	....
Member Prof. Dr. Serap SAFRAN Ankara University	....
Member Prof. Dr. Gürcan YILDIRIM Bolu Abant İzzet Baysal University	....

Institute of Graduate Studies Approval

Prof. Dr. İbrahim KÜRTÜL
Director of Institute of Graduate Studies

ETHICAL DECLARATION

In this thesis dissertation that was properly prepared according to the Thesis Writing Rules of Bolu Abant İzzet Baysal University of the Institute of Graduates Studies, I hereby declare that;

- All data, information, and documents presented in the thesis were obtained in accordance with the academic and ethical rules,
- All data, documents, assessments, and results were presented in accordance with the scientific ethical and moral rules,
- All works that were benefitted in the thesis were appropriately cited,
- No alteration was made in the data used,
- Study presented in this thesis is original,

Otherwise, I declare that I accept the loss of all my rights in case any contradiction that may arise against me.

The similarity rate obtained by using the Turnitin program, a plagiarism detection software, is within the limits approved by the University Senate.

……………………………..

BAYRAM ALBAYRAK

ABSTRACT

SUPERCONDUCTING JOINT STUDIES OF IRON SHEATHED MgB_2 ROUND WIRES BY INDUCTION HEATING METHOD.
MSC THESIS
BAYRAM ALBAYRAK
BOLU ABANT IZZET BAYSAL UNIVERSITY
INSTITUTE OF GRADUATE STUDIES
DEPARTMENT OF PHYSICS
(SUPERVISOR: PROF. DR. MUSTAFA AKDOĞAN)

BOLU, OCTOBER 2024
XV + 63 pages

In this study, we investigated and observed the applicability of the ever-present superconducting junction with iron-sheathed in-situ MgB_2 wires by induction annealing. Within the scope of the study, we fabricated in-situ MgB_2/Fe wires with a diameter of 1.8 mm using the PIT method, sealed both ends of the pieces we cut from these wires with a mechanical press, and annealed them at 900 degrees in the induction facility to form a superconducting phase. We interpreted the results obtained by performing the R-T and I-V characteristics as well as SEM and EDS analyzes of the samples obtained. As a result of this study, we found that superconducting joints in MgB_2/Fe can be formed by induction annealing in a very short time (about 1 minute) and with very low energy consumption. The results we obtained shed light on the applicability of this method to different metal structures with different induction frequencies.

KEYWORDS: Superconducting Joint, Powder in Tube (PIT), MgB_2, Induction, In-situ.

ÖZET

DEMİR KILIFLI MgB_2 YUVARLAK TELLERİN İNDÜKSİYON ISITMA YÖNTEMİ İLE SÜPERİLETKEN EKLEM ÇALIŞMALARI
YÜKSEK LİSANS TEZİ
BAYRAM ALBAYRAK
BOLU ABANT İZZET BAYSAL ÜNİVERSİTESİ
LİSANSÜSTÜ EĞİTİM ENSTİTÜSÜ
FİZİK ANABİLİM DALI
(TEZ DANIŞMANI: PROF. DR. MUSTAFA AKDOĞAN)

BOLU, EKİM - 2024
XV + 63 sayfa

Bu çalışma ile güncelliğini daima koruyan süperiletken eklem konusunun demir kılıflı in-situ MgB_2 tellere indüksiyon tavlama ile uygulanabilirliğini araştırdık ve gözlemledik. Çalışma kapsamında PIT yöntemi ile 1,8 mm çapa sahip in-situ MgB_2/Fe teller üreterek bu tellerden kestiğimiz parçaların her iki ucunu mekanik pres aracılığıyla mühürleyip indüksiyon sisteminde 900 ℃'de süperiletken faz oluşturma tavalamalarını gerçekleştirdik. Elde edilen numunelerin R-T, I-V karakteristikleri ve SEM, EDS analizlerini gerçekleştirerek elde edilen sonuçları yorumladık. Bu çalışma sonucunda indüksiyon tavlama yöntemi ile in-situ MgB_2/Fe'ye çok kısa sürede (1 dakika gibi) ve çok düşük enerji harcayarak süperiletken eklem oluşturulabileceğini ortaya koyduk. Elde ettiğimiz sonuçlar bize bu yöntemin farklı metal yapılara farklı indüksiyon frekansları ile de uygulanabilirliğine ışık tutmuştur.

ANAHTAR KELİMELER: Süperiletken Eklem, Tüp içerisinde Toz (TIT), MgB_2, İndüksiyon, Yerinde faz oluşturma.

TABLE OF CONTENTS

Page

LIST OF FIGURES

Page

LIST OF TABLES

LIST OF PHOTOS

Page

LIST OF ABBREVIATIONS AND SYMBOLS

°C	: Degrees Celsius
A	: Ampere
AC	: Alternative Current
Al	: Aluminum
BCS	: Bardeen-Cooper-Schrieffer
CHPD	: Cold High Presssure Densification
cm	: Centimeter
DC	: Direct Current
EDS	: Energy Dispersive Spectroscopy
Hc	: Critical magnetic field
H_{c1}	: Lower critical field
H_{c2}	: Upper critical field
HIP	: High Isostatic Pressure
HTS	: High Temperature Superconductors
I_c	: Critical current
IMD	: Internal Magnesium Diffusion
J_c	: Critical current density
J_{ce}	: Engineering critical current density
K	: Kelvin
LTS	: Low Temperature Superconductors
mm	: Milimeter
MRI	: Magnetic Resonance Imaging
NbTi	: Niobium-titanium
Pb	: Lead
PIT	: Powder In Tube
PVZ	: Pavezyum
R	: Resistance
SEM	: Scanning Electron Microscope
Sn	: Tin
T	: Tesla
T_c	: Critical temperature
V	: Voltage

XRD : X-ray Diffraction

YBCO : Yttrium barium copper oxide

ACKNOWLEDGEMENT

The author would like to express his deepest gratitude to his master of science (MSc) supervisor Prof. Dr. Mustafa AKDOĞAN for his valuable efforts in the preparation of this thesis.

1. INTRODUCTION

Superconductivity is a fascinating phenomenon observed in certain materials at extremely low temperatures, allowing them to conduct electric current with zero electrical resistance. This unique property has numerous practical applications, making it a subject of significant scientific interest.

The discovery of superconductivity dates back to 1911 when Kamerlingh Onnes observed this phenomenon in mercury at liquid helium temperatures. This breakthrough marked the beginning of the field of superconductivity.

Superconductors are characterized by a critical temperature (T_c) below which they exhibit zero electrical resistance. This critical temperature varies depending on the material; some superconductors require extremely low temperatures near absolute zero, while others can achieve superconductivity at relatively higher temperatures.

One of the striking features of superconductors is the Meissner effect. When a superconductor is cooled below its critical temperature and a magnetic field is applied, the magnetic field is expelled from the interior of the material. This allows for levitation and other fascinating applications.

Superconductivity finds numerous practical uses, such as in high-speed magnetic levitation trains (Maglev trains), magnetic resonance imaging (MRI) machines for medical imaging, particle accelerators in high-energy physics experiments, electrical power transmission through superconducting cables with minimal energy loss (Ballarino et al., 2016; Kostyuk et al., 2012), wind turbine generators for the wind power saving (Kalsi, 2014; Magnusson et al., 2018, 2021), superconducting energy storage (Magnetic energy storage, SMES) (Kwon et al., 2023; Morandi et al., 2017, 2023), fault current limiters (Norris et al., 1997; Pei et al., 2015), superconducting electronics like SQUIDs and sensors (Drung et al., 2007; Hao et al., 2005).

The physical basis of superconductivity is explained by two key concepts: Cooper pairs and the Meissner effect. Cooper pairs are formed when electrons in the material interact with lattice vibrations, resulting in pairs of electrons with opposite spins and momenta. These pairs move through the lattice without scattering, leading to zero resistance. The Meissner effect is responsible for the expulsion of magnetic fields from the interior of the superconductor, creating perfect diamagnetism. This effect allows for various practical applications, including levitation. Furthermore, the BCS (Bardeen-Cooper-Schrieffer) theory, proposed in 1957, provides a microscopic explanation for superconductivity in conventional superconductors like MgB_2. According to the BCS theory, Cooper pairs are formed due to an attractive interaction between electrons mediated by lattice vibrations.

MgB_2, a conventional superconductor, exhibits superconductivity at relatively high temperatures, up to 39 Kelvin, making it a promising material for various applications (Nagamatsu et al., 2001). (Choi & Lee, 2022; Egilmez et al., 2006; Matsumoto et al., 2003) Its unique crystal structure and electron-phonon interactions contribute to its superconducting properties.

Various methods for the production of MgB2 wires can be found in the inliterature, such as PIT (powder in tube)(Akdoğan et al., 2017; Aldica et al., 2018; Kodama et al., 2019), PeIT (pellet in tube)(Karaboğa et al., 2018), IMD (Internal Magnesium Diffusion)(Kováč et al., 2018), CTFF (continuous tube filling and forming)(Ma et al., 2008; Suo et al., 2007), MMC (metal matrix composite), HIP (High Isostatic Pressure)(Gajda et al., 2016), and CHPD (Cold High Pressure Densification)(Flükiger et al., 2012; Senatore et al., 2011). Each method has advantages and disadvantages, but we used the PIT method in this work. As for the precursor material, there are two main methods to prepare the MgB2 structure: in-situ (Akdoğan et al., 2015; Ma et al., 2008; Suo et al., 2007) and ex-situ (Aldica et al., 2018; S. K. Chen et al., 2005) reactions. In this study (the in-situ method was preferred), after preparing the iron sheathed Mg+2B powder mixture obtained by the PIT method, the desired wire diameter was obtained by drawing until it was reduced from 12 mm outer diameter to 1.8 mm outer diameter by using dies with different diameters. Pieces about 10 cm long were cut from the wire. After the two ends of the samples were sealed with a mechanical press, the resistance-temperature (R-T), current-voltage (I-V), SEM and EDS analyzes (Nagoshi & Sato, 2014) were performed after the samples were annealed at 900°C for 1 to 10 minutes in the induction heating system under argon flow in the quartz tube.

Induction equipment is widely used in industry for surface hardening, melting, brazing and welding, annealing, cooking, plastics processing, pyrolysis and appropriate heating of ferrous and non-ferrous precious metals. In this study, we developed an induction coil system with a frequency of 100 kHz (with a maximum power of 1 kW) by procuring the necessary parts in our own laboratory. These included a 500 W power supply, a 1.2 kW voltage amplifier, a digital multimeter and an aquarium water pump. Induction annealing was used in all phases of wire production, both as stress relief annealing and as phase formation annealing.

The main topic of the work relates to the superconductor joint, which is still under development in today's literature (P. Chen et al., 2017; Guven et al., 2024; Mukoyama et al., 2018; Patel et al., 2015, 2021, 2024). Especially when it comes to the production of kilometer- long superconductor wires or tapes, the superconductor joint comes to the fore. One example: There are about 40 km of superconductor wire in an MRI system. If we assume that we produce this wire using the PIT method, both the starting material and the industrial systems to be used take up a lot of space and are costly. Instead, the wires to be produced in shorter pieces can be joined together by a superconductor joint and wires of the desired length can be obtained. However, especially when in-situ MgB_2 superconductor wires are considered, the phase formation annealing of these wires requires a lot of energy and takes a lot of time in today's furnaces, making it costly. Based on this idea, we came up with a solution to the current problem: why not make joints with induction annealing? Based on this idea, we carried out the joint study on the in-situ MgB_2 wires we produced. We used the induction system previously developed by Prof. Dr. Mustafa AKDOĞAN for Ahmed Rajab Ahmed's master's thesis.

2. AIM AND SCOPE OF THE STUDY

This study focuses on combining MgB_2 superconductor wires with the induction heating method to create strong and efficient connections between different sections of MgB_2 wires, while maintaining their superconducting properties. This is important for applications that require longer wires or complex setups. In practical use, superconducting wires need to be joined to form continuous circuits or connect various parts of a system. Achieving these connections without losing the superconducting qualities of the wires is crucial for system performance and efficiency. Induction heating is chosen for this task due to several benefits:

Quick and Targeted Heating: Induction heating heats only the focused area quickly, reducing the risk of damage to the rest of the wire.

Precision Control: This method allows for precise temperature control, ensuring the joint is heated properly without overheating.

Non-Contact Process: As a non-contact method, induction heating prevents contamination or damage to the wire.

Scalability: Induction heating can be scaled up for industrial production of superconducting wires with reliable joints.

By using this method, engineers can create high-performance joints in MgB_2 superconductor wires, supporting practical applications like high-field magnets, power transmission cables, and fault current limiters. These applications can lead to better energy transmission and advanced electronic devices.

In summary, this study aims to enhance the practical use of superconductors through the combination of MgB_2 wires and induction heating, promoting energy-efficient technologies across various fields.

3. SUPERCONDUCTIVITY

Superconductivity is a phenomenon observed in certain materials at very low temperatures, where they can conduct electric current with zero electrical resistance. In other words, superconductors allow the flow of electric current without any energy loss due to resistance, which is the main cause of energy wastage in conventional conductors.

The superconductivity phenomenon was first discovered by Kamerlingh Onnes on mercury at liquid helium temperature in 1911 (Onnes, 1911). This observation marked the beginning of the field of superconductivity.

Superconductors are characterized by a critical temperature, often referred to as T_c, below which they exhibit zero electrical resistance. At temperatures above T_c, they behave like normal conductors. The critical temperature varies depending on the material; some superconductors require extremely low temperatures near absolute zero, while others can exhibit superconductivity at relatively higher temperatures.

One of the key features of superconductors is the Meissner effect. When a superconductor is cooled below its critical temperature and a magnetic field is applied to it, the magnetic field is expelled from the interior of the material. This causes the superconductor to exhibit perfect diamagnetism, where it repels the magnetic field lines. This effect allows for levitation and other fascinating applications.

Superconductivity has numerous practical applications. Some of the notable ones include:

1. High-speed magnetic levitation trains (Maglev trains): Superconducting magnets enable the trains to float above the tracks, reducing friction and allowing for faster speeds.
2. Magnetic resonance imaging (MRI): Superconducting magnets generate the intense magnetic fields necessary for medical imaging.
3. Particle accelerators: Superconducting magnets are used to steer and control the particle beams in high-energy physics experiments.
4. Electrical power transmission: Superconducting power cables can transmit electricity with minimal losses over long distances.
5. Energy storage: Superconducting materials can store electrical energy with high efficiency.

While superconductivity has been mainly observed at low temperatures, researchers continue to explore and discover new materials that exhibit superconductivity at higher temperatures. This field of high-temperature superconductivity holds great promise for future technological advancements and energy-efficient applications.

The physical basis of superconductivity can be explained by two key concepts: Cooper pairs and the Meissner effect.

3.1 Cooper Pair

The term "Cooper pair" refers to a phenomenon in condensed matter physics known as Cooper pairing, which occurs in certain superconducting materials. Superconductivity is a state in which a material can conduct electric current without any resistance.

Cooper pairs are pairs of electrons that form due to an interaction mediated by the lattice vibrations (phonons) in the material. Normally, electrons in a metal repel each other due to their mutual electrical charge, making it difficult for them to move through the material without scattering off impurities or lattice defects, resulting in electrical resistance.

In a superconducting material, however, the lattice vibrations create an attractive interaction between two electrons with opposite spins and momenta. This attractive force overcomes the usual repulsion, causing the electrons to form pairs known as Cooper pairs. These pairs have a net spin of zero, which is one of the requirements for superconductivity according to the Bardeen-Cooper-Schrieffer (BCS) theory.

The formation of Cooper pairs allows for the phenomenon of superconductivity to occur. When a material is cooled below its critical temperature, the Cooper pairs can move freely through the lattice without scattering, resulting in the flow of electric current without resistance. This property has numerous practical applications, such as in the development of highly efficient power transmission lines, magnetic resonance imaging (MRI) machines, and particle accelerators.

3.2 Meissner Effect

The Meissner effect (Figure 3.1), also known as the Meissner-Ochsenfeld effect, is a fundamental principle in physics that describes the expulsion of magnetic fields from a superconductor when it undergoes a phase transition to a superconducting state. The exclusion of the magnetic field from the interior of a superconductor is known as the Meissner effect (Schmidt, 1997) It is named after the German physicists Walther Meissner and Robert Ochsenfeld, who discovered this phenomenon in 1933.

When a material becomes superconducting at or below a certain critical temperature, it exhibits zero electrical resistance and perfect diamagnetism. In the presence of an external magnetic field, the Meissner effect causes the superconductor to actively expel magnetic flux from its interior, resulting in a complete exclusion of magnetic fields from the material.

The expulsion of magnetic fields occurs due to the formation of superconducting current loops, called persistent currents, on the surface of the superconductor. These persistent currents generate an equal and opposite magnetic field that cancels out the applied magnetic field within the superconductor. As a result, the magnetic field is confined to the exterior of the superconductor.

The Meissner effect is responsible for some remarkable properties of superconductors, such as their ability to levitate in the presence of a magnetic field. When a superconductor is placed near a magnet, the repulsion between the expelled magnetic field and the applied magnetic field causes the superconductor to float or "levitate" above the magnet, a phenomenon known as quantum levitation.

The Meissner effect is a crucial characteristic of superconductivity and has significant applications in various fields, including magnetic levitation, superconducting magnets, and high-speed transportation systems like maglev trains. It also plays a vital role in the development of technologies such as superconducting quantum interference devices (SQUIDs) used in sensitive magnetic field measurements and superconducting radio frequency cavities employed in particle accelerators.

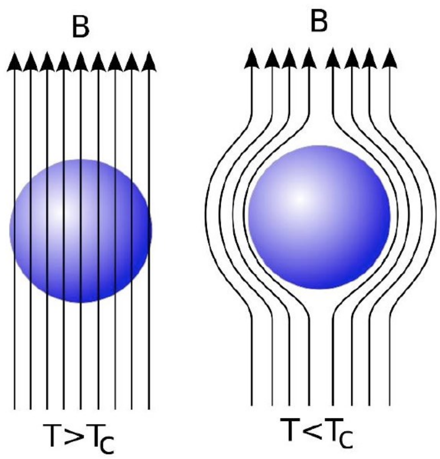

Figure 3.1 Diagram of the Meissner effect. Flux lines are excluded from a superconductor when it is below its critical temperature.

3.3 Type-I and Type-II Superconductors and MgB_2

Type-I and Type-II superconductors (Figure 3.2) are two distinct categories of materials based on their behavior in the presence of a magnetic field. The classification is determined by their critical magnetic field (H_c) and the response to increasing magnetic field strength. MgB_2 has both type-I and type-II superconducting behaviors, offering a unique characteristic that distinguishes it from many other superconductors. The type-I superconductivity in MgB_2 is attributed to the π-bands, while the type-II superconductivity arises due to the σbands (Moshchalkov V, 2009). This dual behavior makes MgB_2 an intriguing and versatile material for various applications, especially in magnetic fields.

In type-I superconductors, the magnetic field is completely expelled from the material below a critical magnetic field value, and it exhibits a sudden transition from the superconducting to the normal state. On the other hand, type-II superconductors allow partial penetration of the magnetic field even below their critical magnetic field. They exhibit a mixed state where magnetic flux lines penetrate the material in quantized units called fluxoids. Type-II superconductors are more technologically significant due to their ability to carry higher currents and withstand stronger magnetic fields, making them suitable for various practical applications.

The unique combination of type-I and type-II superconductivity in MgB_2 highlights its exceptional electronic and structural properties, offering promising opportunities for research and technological advancements. Researchers continue to explore and understand the underlying mechanisms of this fascinating material, further enriching the field of superconductivity and opening doors to innovative applications in various industries.

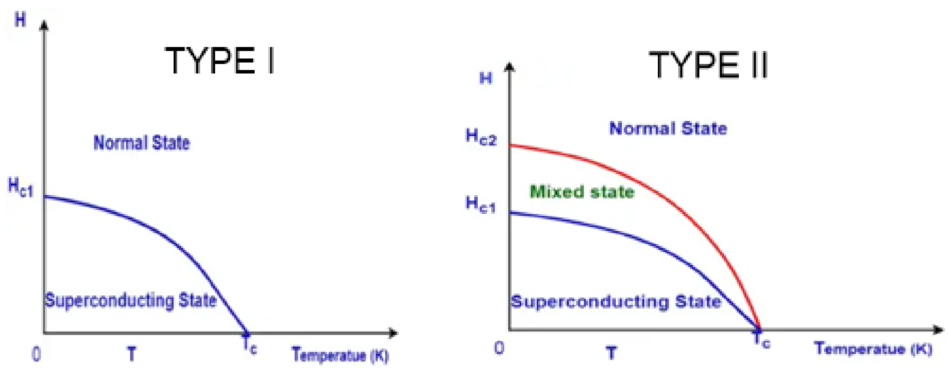

Figure 3.2 Critical Field vs. Temperature graphs of the Type I and the Type II superconductors.

3.3.1 Type-I Superconductors:

In Type-I superconductors, superconductivity occurs in a narrow range of temperatures close to absolute zero (usually below 10 Kelvin). They are generally elemental superconductors like lead (Pb), tin (Sn), and aluminum (Al).

Type-I superconductors have a single critical magnetic field (H_c) at which they transition from the superconducting state to the normal state. When the external magnetic field exceeds the critical field, superconductivity is completely destroyed, and the material behaves like a normal conductor with electrical resistance.

In the superconducting state, Type-I superconductors expel all magnetic flux (Meissner effect) from their interior. They do not allow magnetic field lines to penetrate their bulk, resulting in complete diamagnetism. As a result, Type-I superconductors cannot be used to trap magnetic fields effectively or carry high magnetic fields in practical applications.

The Meissner effect in Type-I superconductors is stable as long as the applied magnetic field is below the critical field. If the magnetic field exceeds the critical field, the superconductor undergoes a sudden transition to the normal state with complete flux expulsion.

Due to their limited practical applications and the Meissner effect's sensitivity to external magnetic fields, Type-I superconductors are less commonly used in technology and engineering.

3.3.2 Type-II Superconductors:

Type-II superconductors have a broader range of superconducting temperatures, which can extend to higher temperatures than Type-I materials. They are often composed of compounds or alloys, such as niobium-titanium (NbTi) or yttrium barium copper oxide (YBCO).

Type-II superconductors have two critical magnetic fields: the lower critical field (H_{c1}) and the upper critical field (H_{c2}). The lower critical field is the threshold below which the material transitions to the superconducting state, and the upper critical field is the limit above which superconductivity is destroyed.

In the superconducting state, Type-II superconductors allow partial penetration of magnetic field lines into their bulk. This partial flux penetration forms quantized vortices or flux lines. The vortices can move within the material, leading to a mixed state where superconductivity coexists with vortices.

The mixed state of Type-II superconductors allows them to carry much higher magnetic fields than Type-I superconductors. They are used extensively in applications requiring strong magnetic fields, such as superconducting magnets for MRI machines, fusion reactors, and particle accelerators.

Type-II superconductors are also more robust and less sensitive to external magnetic fields compared to Type-I superconductors. Their ability to handle higher magnetic fields and still maintain superconductivity makes them more practical for a wide range of technological applications.

In summary, Type-I and Type-II superconductors exhibit different responses to magnetic fields, have distinct critical magnetic fields, and vary in their practical applications. While Type-I superconductors exhibit the Meissner effect and have a single critical field, Type-II superconductors allow partial flux penetration, have two critical fields, and are more suitable for high-field applications.

4. MAGNESIUM DIBORIDE SUPERCONDUCTOR

4.1 Exploration of MgB_2

The superconductivity of MgB_2 was discovered by Akimitsu Jun and his team in 200 (Nagamatsu et al., 2001) 1 although MgB_2 was known since 1950. It belongs to the class of conventional superconductors, which means that its behavior can be explained by the conventional theory of superconductivity proposed by Bardeen, Cooper, and Schrieffer (BCS theory).

The unique aspect of MgB_2 is its relatively high superconducting transition temperature (T_c) compared to other conventional superconductors. While most elemental superconductors have T_c values below 10 Kelvin, MgB_2 exhibits superconductivity at temperatures up to 39 Kelvin (-234 degrees Celsius or -389 degrees Fahrenheit). Although this might not seem high compared to some high-temperature superconductors, it is significant for a conventional superconductor.

The crystal structure of MgB_2 consists of alternating layers of magnesium and boron atoms. The boron atoms form a hexagonal lattice, and each boron atom is surrounded by six magnesium atoms, which form a honeycomb-like structure. Superconductivity with a high transition temperature is achieved due to strong electron-phonon interactions with high vibrational frequencies of light B atoms in MgB_2 (Ravindran et al., 2001). The superconductivity in MgB_2 arises due to the interaction between electrons and the vibrations of the boron atoms, known as phonons. These phonons facilitate the formation of Cooper pairs, which are responsible for carrying electrical current without resistance.

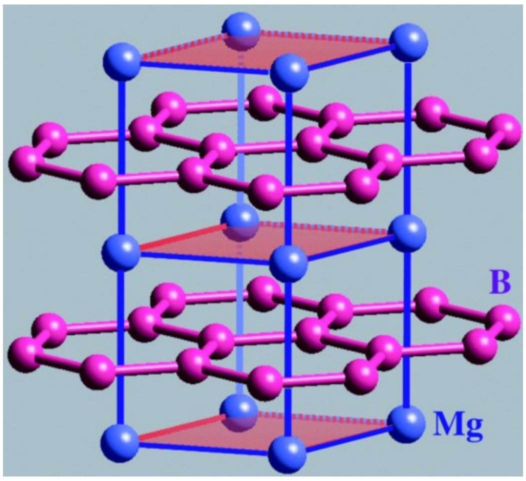

Figure 4.1 The crystal structure of MgB_2

MgB_2 has been fabricated into various shapes such as bulks (Wang Qingyang Y. G., 2011), single crystals thin films, wires (Wang Qingyang Y. G., 2012) and tapes (Liu Guoqing, 2011) (Sun Yuyan, 2012), etc. An abundant published research results revealed the great interest community in this materials.

MgB_2 has shown promise for various applications due to its relatively high critical temperature and relatively low fabrication costs compared to some high-temperature superconductors. It has been used in the development of superconducting wires, cables, and magnets for applications such as energy transmission, magnetic resonance imaging (MRI), and particle accelerators. However, further research is still ongoing to improve the material's performance and explore its full potential.

4.2 Comparison of MgB_2 with HTS

Superconductivity with a high transition temperature is achieved due to strongelectron-phonon interactions with high vibrational frequencies of light B atoms in MgB_2 (Ravindran P, 2001) MgB_2 is a unique superconducting material that exhibits properties of both low-temperature superconductors (LTS) and high-temperature superconductors (HTS). To provide a clearer comparison, we will focus on MgB_2 in relation to typical HTS materials like yttrium barium copper oxide (YBCO) and bismuth strontium calcium copper oxide (BSCCO). Let's identify the advantages and disadvantages of MgB_2 compared to HTS:

4.2.1 Advantages of MgB_2 Over HTS

Relatively High Critical Temperature (Tc): MgB_2 has a critical temperature of around 39 Kelvin, which is significantly higher than most LTS materials and closer to the temperature range of some HTS materials. This allows for the use of more accessible and cost-effective coolants like liquid nitrogen.

Cost-Effectiveness: The materials used in MgB_2, magnesium, and boron, are abundant and relatively low-cost compared to some rare and expensive elements found in certain HTS materials. This makes MgB_2 a more economical choice for large-scale applications.

Scalability: MgB_2 is relatively easier to produce in the form of wires and tapes compared to some HTS materials. This makes it more practical for developing long lengths of superconducting wires, which are essential for various technological applications, such as power transmission cables and high-field magnets.

Low Anisotropy: MgB_2 exhibits lower anisotropy compared to some HTS materials, meaning its superconducting properties are more isotropic and less dependent on the direction of an applied magnetic field. This makes it easier to manufacture practical superconducting devices.

Simple Crystal Structure: MgB_2 has a relatively simple crystal structure compared to some complex HTS materials, which simplifies the manufacturing process and makes it easier to control the material's properties.

4.2.2 Disadvantages of MgB_2 Over HTS

Critical Current Density (J_c): One of the main challenges with MgB_2 is achieving high critical current densities (J_c) to carry higher current loads without losing superconductivity. Some HTS materials, like YBCO, can achieve higher J_c values, especially in the presence of high magnetic fields.

Flux Pinning: MgB_2 has relatively weaker flux pinning compared to certain HTS materials. Flux pinning is essential for stabilizing the superconducting state in the presence of magnetic fields, and higher pinning forces result in better performance.

Intrinsic Brittle Nature: MgB_2 is inherently brittle, which can make it more susceptible to mechanical stress and strain during fabrication and use. Some HTS materials exhibit better mechanical properties, making them more durable in certain applications.

High Magnetic Field Applications: While MgB_2 has a higher critical magnetic field (H_c) than LTS materials, it may not be as suitable as some HTS materials for extreme high-field applications like superconducting magnets used in fusion research.

In conclusion, MgB_2 offers a unique set of advantages due to its relatively high critical temperature, cost-effectiveness, and scalability. However, it also has some limitations, particularly in achieving high critical current densities and flux pinning compared to certain HTS materials. Despite these challenges, ongoing research and development efforts are continually improving MgB_2's properties and expanding its applications in various superconducting technologies.

4.3 Comparison of MgB_2 with LTS

MgB_2 (magnesium diboride) is a type of superconductor that exhibits properties of both low-temperature superconductors (LTS) and high-temperature superconductors (HTS). Let's compare MgB_2 with typical LTS materials like niobium-titanium (NbTi) and niobium-tin (Nb_3Sn) and identify the advantages and disadvantages of MgB_2:

4.3.1 Advantages of MgB_2 Over LTS

Higher Critical Temperature (T_c): MgB_2 has a relatively higher critical temperature (around 39 Kelvin) compared to LTS materials like NbTi (around 10 Kelvin) and Nb_3Sn (around 18 Kelvin). This higher T_c allows MgB_2 to operate at less extreme cryogenic temperatures, making it more practical for certain applications.

Cost-Effectiveness: The materials used in MgB_2, magnesium, and boron, are abundant and relatively low-cost compared to the expensive niobium used in NbTi and Nb_3Sn. This makes MgB_2 a more economical choice for large-scale applications.

Scalability: MgB_2 is easier to produce in the form of wires and tapes compared to LTS materials. This makes it more practical for developing long lengths of superconducting wires, which are essential for various technological applications, such as power transmission cables and high-field magnets.

Simple Fabrication: The fabrication process for MgB_2 is relatively simpler compared to LTS materials, which can involve complex heat treatments and multiple steps. This simplicity allows for faster and more cost-efficient manufacturing.

Lower AC Losses: MgB_2 exhibits lower alternating current (AC) losses compared to some LTS materials. This property is crucial for certain applications, such as power transmission, where minimizing energy losses is essential.

4.3.2 Disdvantages of MgB_2 Over LTS

Lower Critical Current Density (J_c): One of the main challenges with MgB_2 is achieving high critical current densities (J_c) to carry higher current loads without losing superconductivity. LTS materials like Nb_3Sn can achieve higher Jc values, especially in the presence of high magnetic fields.

Flux Pinning: LTS materials often exhibit better flux pinning, which is essential for stabilizing the superconducting state in the presence of magnetic fields. MgB_2 has relatively weaker flux pinning, limiting its performance in high-field applications.

Intrinsic Brittle Nature: MgB_2 is inherently brittle, which can make it more susceptible to mechanical stress and strain during fabrication and use. LTS materials tend to have better mechanical properties, making them more durable in certain applications.

Low Critical Magnetic Field (H_{c1}): The lower critical magnetic field (H_{c1}) of MgB_2 compared to LTS materials can limit its suitability for high magnetic field applications.

In summary, MgB_2 offers advantages over LTS materials, such as a higher critical temperature, cost-effectiveness, scalability, and lower AC losses. However, it faces challenges in achieving high critical current densities and flux pinning, which are strengths of some LTS materials like Nb_3Sn. Despite these limitations, MgB_2 continues to be researched and developed for various superconducting applications, with ongoing efforts to enhance its performance and expand its practical use.

4.4 The Fabrication Methods of MgB_2 Ssuperconducting Wires

MgB_2 In the realm of superconducting wire fabrication for MgB_2, various techniques have been explored, including the Powder-in-Tube (PIT) method, the In Situ Magnesium Diboride (IMD) method, and the Hot Isostatic Pressure (HIP) and Cold High-Pressure Densification (CHPD) methods. Each method exhibits unique advantages and challenges in achieving optimal core density and superconducting properties for these wires, catering to diverse research and practical applications. Recently, a novel approach known as the Pellet-in-Tube (PeIT) method has been introduced, offering impressive initial filling density and enhanced uniformity, making it particularly promising for the production of long-scale wires.

4.4.1 Powder in Tube Method (PIT)

Only several months after the discovery of superconductivity in MgB_2, the first MgB_2 wires were prepared by Canfield et al (Canfield et al., 2001). The fabrication method of MgB_2 superconducting wires typically involves a powder-in-tube (PIT) technique or Continuous Tube Filling and Forming (CTFF) methods (S. K. Chen et al., 2005; Collings et al., 2002) . This method allows for the production of long, flexible wires that exhibit superconductivity at relatively high temperatures.

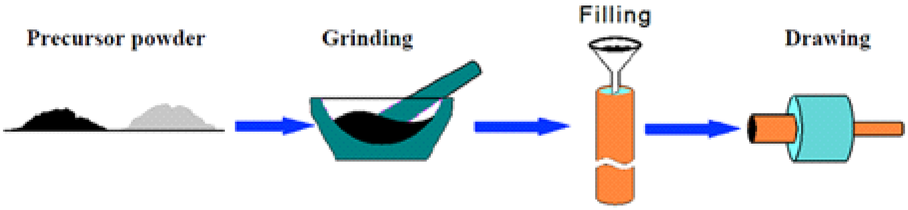

Figure 4.2 Schematic diagram of the Powder in tube process (PIT)

Here are the general steps involved in the fabrication of MgB_2 superconducting wires:

1. Powder Preparation: High-purity magnesium (Mg) and boron (B) powders are prepared separately. The powders are typically mixed in a specific stoichiometric ratio to achieve the desired composition of MgB_2. It is important to use high-quality powders to ensure the wire's performance.
2. Tube Preparation: A metallic tube, often made of stainless steel or a nickel-based alloy, is selected as the substrate for the superconducting wire. The tube's inner surface is usually coated with a thin layer of a suitable barrier material, such as tantalum or niobium, to prevent chemical reactions between the MgB_2 and the substrate.
3. Powder Filling: The Mg and B powders are mixed thoroughly and then packed inside the prepared tube. The tube is typically filled using a mechanical or pneumatic method, ensuring uniform distribution of the powder mixture.
4. Tube Sealing: The open ends of the tube are sealed using a suitable method, such as welding or crimping, to enclose the powder mixture

securely. This step helps maintain the integrity of the wire during subsequent processing steps.

5. Wire Drawing: The sealed tube containing the MgB_2 powder is reduced in size through a series of wire drawing steps. The tube is passed through a series of dies with decreasing diameters, resulting in a continuous wire with the desired dimensions. The wire is typically drawn several times to achieve the desired final diameter.

Table 4.1 Drawing steps for the MgB_2/Fe PIT wire.

Steps	Diameters of dies (mm)	Steps	Diameters of dies (mm)
1	12.00	31	5.30
2	11.30	32	5.15
3	11.00	33	5.00
4	10.80	34	4.85
5	10.65	35	4.70
6	10.50	36	4.50
7	10.30	37	4.45
8	10.00	38	4.30
9	9.80	39	4.25
10	9.50	40	4.10
11	9.20	41	3.95
12	9.10	42	3.85
13	8.90	43	3.75
14	8.60	44	3.72
15	8.50	45	3.57
16	8.35	46	3.43
17	8.20	47	3.27
18	8.00	48	3.12
19	7.75	49	3.00
20	7.60	50	2.85
21	7.40	51	2.71
22	7.20	52	2.64
23	6.90	53	2.50
24	6.70	54	2.38
25	6.50	Stress relief annealing at 500 °C for 1 minute under Argon atmosphere with Induction heater.	
26	6.30	55	2.21
27	6.20	56	2.10
28	6.10	57	2.00
29	5.90	58	1.90
30	5.50	59	1.80

6. Heat Treatment: The as-drawn wire undergoes a heat treatment process called annealing. This step is crucial for transforming the MgB_2 powder

into a superconducting state with high critical temperature (T_c). The wire is typically heated at a specific temperature for a defined period, often under a controlled atmosphere to avoid oxidation.

7. Optional Sheath Application: In some cases, a protective sheath is applied to the superconducting wire to enhance its mechanical and thermal stability. The sheath material, such as stainless steel or a high-temperature polymer, is chosen to provide adequate protection while minimizing any adverse effects on the superconducting properties.

These steps represent a general outline of the fabrication process for MgB_2 superconducting wires. However, variations in the specific techniques and parameters can exist depending on the particular manufacturing setup and goals of the research or production facility.

4.4.2 IMD Method

The IMD (Internal Magnesium Diffusion) method is a fabrication route used to synthesize magnesium diboride (MgB_2), a high-temperature superconducting material. This method was proposed by Giunchi et al. in a research paper published in 2003 (Giunchi et al., 2003).

In the IMD method, a unique approach is employed to create MgB_2 by inserting a uniform magnesium (Mg) rod into the center of a metallic tube. The gap between the Mg rod and the tube is then filled with boron (B) powder. By subjecting this composite structure to appropriate heat treatment, the Mg and B elements react in situ, forming the MgB_2 compound.

The advantage of the IMD method lies in its simplicity and the relative ease of the fabrication process. It allows for the controlled and uniform distribution of boron within the Mg rod, leading to the formation of high-quality MgB_2 material. Additionally, the IMD method offers a cost-effective way to produce MgB_2, making it a promising option for various research and practical applications.

Researchers and scientists continue to investigate and optimize the IMD method to enhance the properties of MgB_2 and explore its potential in superconducting technologies and other cutting-edge applications.

4.4.3 HIP and CHPD Methods

The densification of the core in PIT (powder-in-tube) MgB_2 wires, concerning grain connectivity and porous structure, has been the subject of extensive research. Various methods have been explored to enhance the core density and optimize the superconducting properties of MgB_2 wires. Two such methods, the hot isostatic pressure (HIP) method and the cold high-pressure densification (CHPD) method, have emerged as prominent techniques in this pursuit.

The hot isostatic pressure (HIP) method, as proposed by Gajda involves subjecting the MgB_2 wire to high pressure and elevated temperature. (Gajda D, 2018) This process significantly increases the core density by enhancing grain connectivity and reducing the porosity of the material. As a result, the superconducting performance is greatly improved. However, a limitation of the HIP method is that it can only be effectively applied to short wire samples due to the constraints of the process.

In contrast, the cold high-pressure densification (CHPD) method, introduced by Hossain, offers a solution for achieving densification at long length scales (Flükiger et al., 2012). This method allows for the compression and densification of the MgB2 core without the need for elevated temperatures. The CHPD method has shown promising results in enhancing the core density and improving the superconducting properties of MgB_2 wires, particularly in longer lengths, making it suitable for various practical applications.

Both the HIP and CHPD methods have contributed significantly to the advancement of MgB_2 wire technology, offering complementary approaches to achieve the desired densification and optimization of superconducting properties.

4.4.4 PeIT Method

Recently, a novel approach to the Pellet-in-Tube (PeIT) method was proposed by Karaboğa et al (Karaboğa et al., 2018). The main objective of this alternative method is to enhance the initial filling density of the in-situ Mg+2B precursor powder within the metallic iron tube, as illustrated in Figure 5 This new technique, known as the pellet-in-tube (PeIT) method, achieves an impressive initial filling density of up to 60% of the theoretical mass density of the MgB_2 phase.

As a result, it represents a significant improvement in achieving higher core density, even though it does not entirely eliminate the formation of a porous structure.

The PeIT method plays a crucial role, especially in the production of long-scale wires, due to the more uniform filling of the starting powder along the tube compared to conventional powder filling methods. This enhanced uniformity in powder distribution contributes to improved grain connectivity and reduces the occurrence of voids or porosity within the wire.

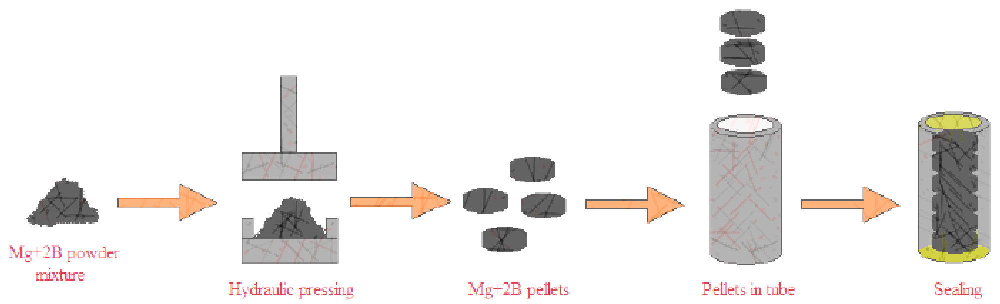

Figure 4.3 In-situ pellet-in-tube (PeIT) method for MgB_2/Fe wire fabrication.

4.5 The Usage Area of MgB_2 Superconducting Wire?

MgB_2 (magnesium diboride) superconducting wire has several usage areas due to its unique properties. Here are some of the main applications:

1. Energy Generation and Transmission: MgB_2 superconducting wire can be used in the construction of high-field magnets for applications such as magnetic resonance imaging (MRI) machines, fusion reactors, and particle accelerators. These magnets require a strong magnetic field, and MgB_2 wires can provide efficient and cost-effective solutions.
2. Power Cables: MgB_2 superconducting wires can be used in power transmission cables to reduce energy loss during transmission. Superconducting cables made with MgB_2 can carry significantly higher amounts of current compared to conventional copper or aluminum cables, reducing energy waste and increasing efficiency.
3. Fault Current Limiters: MgB_2 superconducting wires can be employed as fault current limiters in electrical grids. When a fault occurs, the superconducting wire rapidly transitions to the normal state, effectively limiting the magnitude of the fault current and protecting the grid from damage.
4. Magnetic Levitation: MgB_2 wires can be used in magnetic levitation (maglev) systems for transportation, such as high-speed trains. The superconducting properties of MgB_2 allow for the creation of strong

magnetic fields, enabling the levitation and propulsion of vehicles with minimal friction.

5. Superconducting Electronics: MgB_2 superconducting wires can be utilized in various electronic applications, including superconducting quantum interference devices (SQUIDs), superconducting digital circuits, and superconducting sensors. These technologies benefit from the low electrical resistance and high sensitivity of MgB_2 wires.

It's worth noting that MgB2 superconducting wires are still being researched and developed, and their commercial applications may continue to expand as further advancements are made in the field of superconductivity.

4.6 Superconducting Joint of MgB_2 Wire

Various techniques, such as diffusion splicing, PIT joint, cold welding, soldering, mechanical compression joints, and wire stacking, offer diverse methods to create superconducting joints in MgB2 wires, each with its advantages and limitations. Some superconductor joining methods briefly mentioned and go to my own work.

4.6.1 Diffusion Splicing

Diffusion splicing involves aligning two separate MgB_2 wire segments and heating them to a temperature just below the melting point of MgB_2. The heat causes boron atoms on the wire surfaces to diffuse and mix, creating a solid-state joint. Pressure may be applied during the heating process to ensure good contact between the wire segments. Diffusion splicing can be performed using various heating techniques such as resistance heating, laser heating, or induction heating.

4.6.2 Powder-in-Tube (PIT) Joint

The PIT process, commonly used for fabricating long MgB_2 wires, can also be utilized for creating superconducting joints. In this method, the two wire segments to be joined are placed inside a metallic tube along with a powdered boron source. The tube is then sealed and heated to a high temperature to initiate a chemical reaction between the boron powder and the wire surfaces, resulting in a joint.

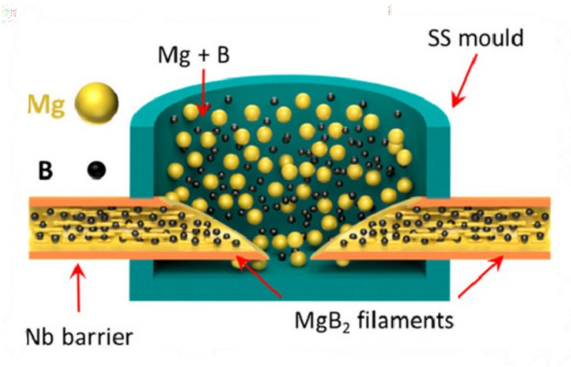

Figure 4.4 PIT method of joint.

4.6.3 Cold Welding

Cold welding is a technique where two clean MgB_2 wire surfaces are mechanically pressed together under high pressure. The pressure causes the metal atoms on the wire surfaces to bond, creating a solid joint. Cold welding is typically performed at room temperature or slightly elevated temperatures without the need for external heat sources.

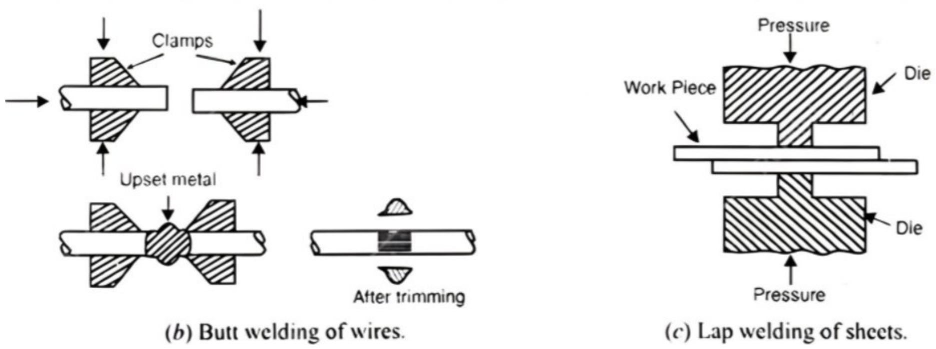

Figure 4.5 Cold welding joint of the wire.

4.6.4 Soldering

Soldering involves using a low-temperature superconducting material (such as Pb-Bi or In-Ag) as a solder to join two MgB_2 wire segments. The solder is heated to its melting point, and when it cools, it forms a bond between the wires.

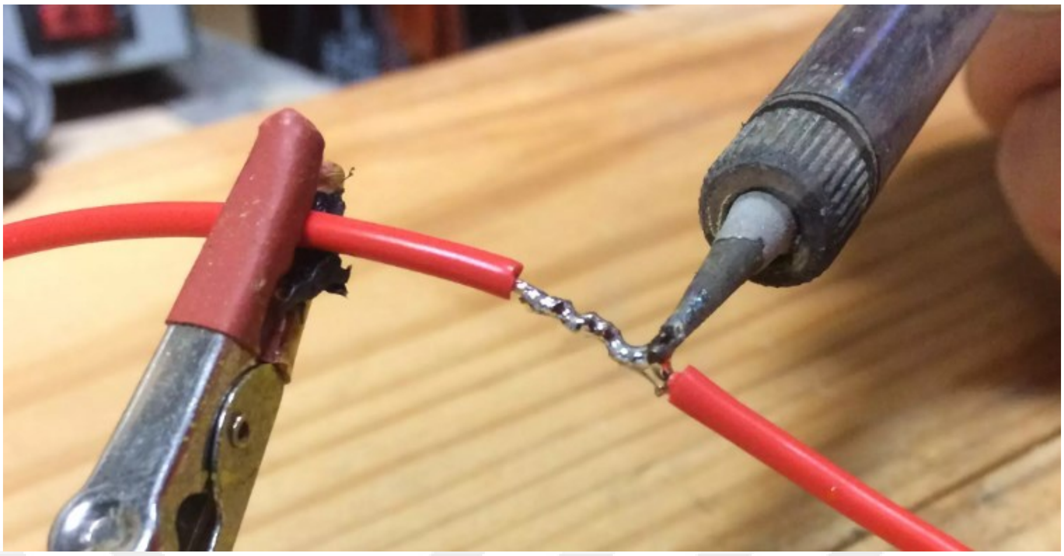

Photo 4.1 Soldering of the wires.

4.6.5 Mechanical Compression Joints

In this method, two MgB_2 wire segments are mechanically compressed using specially designed connectors or clamps to create a joint as shown in Figure 4.6. The pressure ensures good electrical and mechanical contact between the wires.

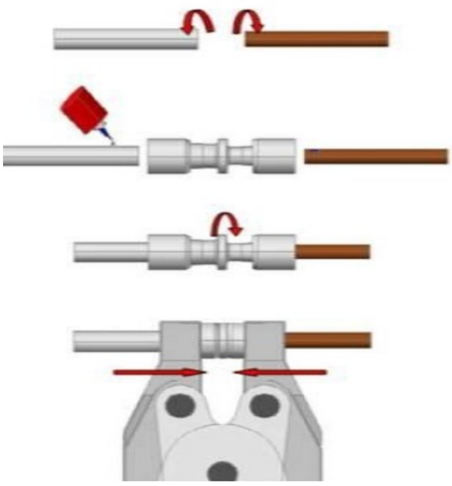

Figure 4.6 Mechanical compression joint.

4.6.6 Wire Stacking

Wire stacking involves layering multiple MgB_2 wires on top of each other to form a joint. The layers are compressed and then heated to form a solid joint.

The choice of the method depends on various factors, such as the specific application, required joint strength, and the type of MgB_2 wire being used. Each method has its advantages and limitations, and ongoing research is focused on developing more efficient and reliable techniques for superconducting joints of MgB_2 wires. One of these studies is the induction heating method that we will work on.

4.6.7 Our Idea Used in This Thesis

Below you can see the picture of the hydraulic hand press (Photo 4.2) we used in our thesis and the schematic representation (Figure 4.7) of how we applied it to the wires:

Photo 4.2 Hydrolic hand press with different perspectives.

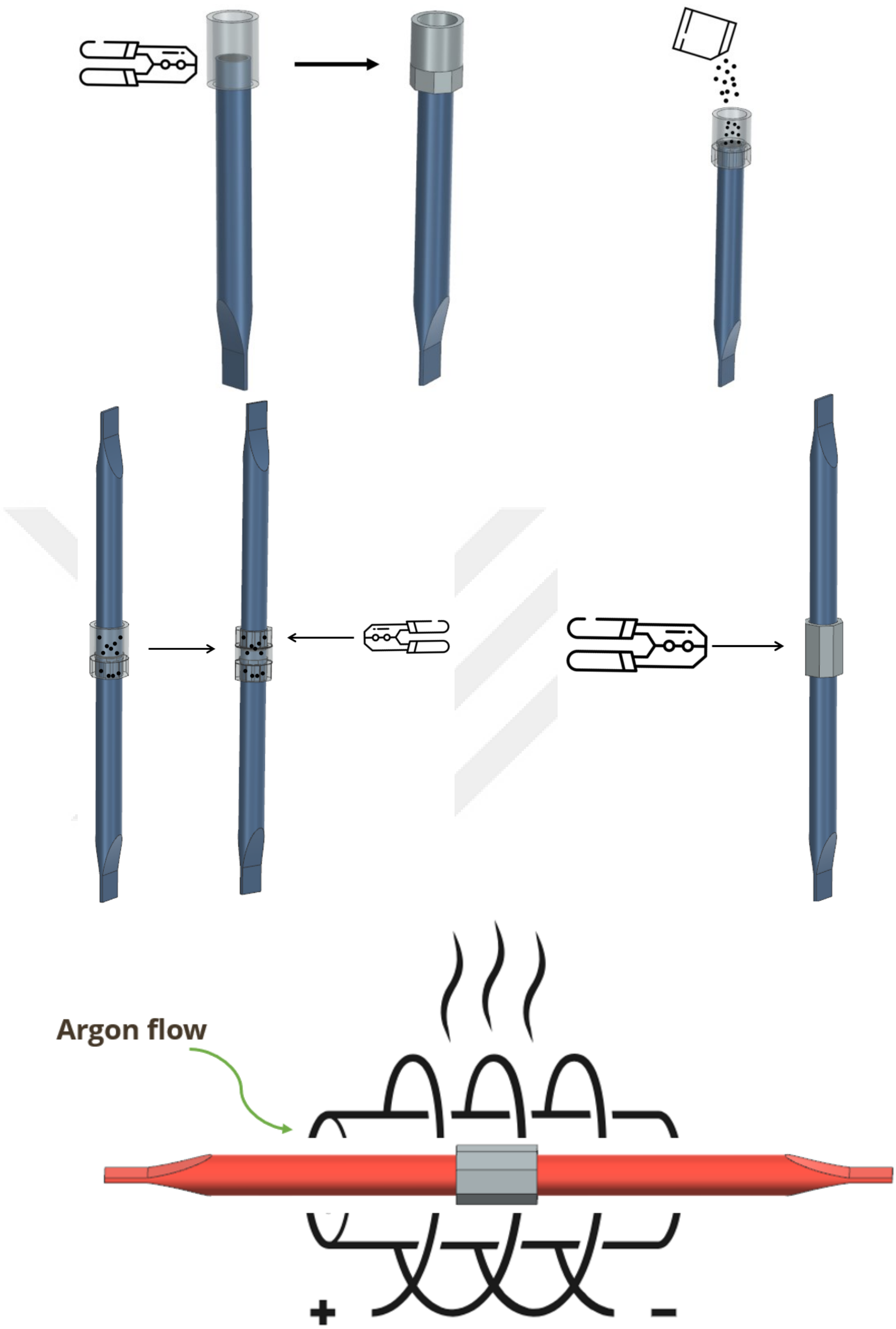

Figure 4.7 Preparation steps of the joint sample and annealing under Argon flow by induction.

5. INDUCTION HEATING

Induction heating is a method of heating an electrically conductive material by using electromagnetic induction to generate heat within the material itself. It relies on the principle of Faraday's law of electromagnetic induction, which states that when a conductor is placed in a varying magnetic field, an electric current is induced in the conductor.

The basic setup of an induction heating system consists of an induction coil, often made of copper tubing, that generates the alternating magnetic field, and a power supply that provides high-frequency electrical current to the coil. When a conductive material (such as metal) is placed within the coil, the alternating magnetic field induces eddy currents in the material, causing it to heat up due to electrical resistance. The heat is generated directly within the material, making induction heating an efficient and controllable heating method.

5.1 Some usage areas of induction heating

Industrial Applications: Induction heating finds widespread use in various industries due to its efficiency and adaptability. Some of the common industrial applications include:

Metal Hardening and Tempering: Induction heating is used to harden and temper steel and other metals, improving their hardness, strength, and wear resistance.

Brazing and Soldering: It is employed to join metal parts using brazing or soldering techniques, ensuring strong, reliable, and clean joints.

Annealing: Induction annealing is used to soften metals for improved machinability or to relieve internal stresses.

Induction Forging: It is employed to heat metal for forging processes, making it easier to shape and deform.

Induction Melting: Induction furnaces are used for melting metals in foundries and metallurgical processes.

Heat Treatment: Induction heating is used in various heat treatment processes like surface hardening, case hardening, and localized heat treatment.

Cooking and Food Industry: Induction cooktops and induction ranges have gained popularity in household kitchens and commercial cooking settings. They offer fast, precise, and energy-efficient cooking by directly heating the cooking vessel through induction.

Semiconductor Industry: In semiconductor manufacturing, induction heating is utilized for processes like wafer annealing and bonding.

Aerospace and Automotive Industry: Induction heating is used for various applications in these industries, such as heat treatment of components and joining of parts.

Electronics Industry: Induction heating is used in soldering and reflow processes for electronic components and PCBs.

5.2 Advantages of induction heating

Energy Efficiency: Induction heating is highly energy-efficient because it directly heats the material without the need for an intermediate heating element. Traditional heating methods, such as gas furnaces or resistive heating, often result in significant heat losses during heat transfer. Induction heating, on the other hand, generates heat within the material itself, minimizing wastage and reducing overall energy consumption.

Rapid and Controlled Heating: Induction heating is known for its fast and controllable heating rates. The heat is generated almost instantly when the material is placed within the magnetic field, allowing for quick processing times. Moreover, the heating intensity can be precisely controlled by adjusting the power supplied to the induction coil, enabling precise temperature control and uniform heating.

Safe and Clean Operation: Induction heating is a safe method as it does not involve an open flame or exposed heating element. The heat is produced directly within the material, eliminating the risk of burns or fires caused by contact with a hot surface. Additionally, since no combustion takes place, there are no harmful emissions or fumes, making it a clean and environmentally friendly heating process.

Selective and Localized Heating: Induction heating offers selective and localized heating, which is particularly advantageous in various applications. By using different coil designs and configurations, it is possible to heat specific areas of a workpiece while leaving other parts unaffected. This capability is crucial for processes such as induction brazing, welding, and heat treating, where precise control over the heated zones is essential.

Consistent and Repeatable Results: The controllable nature of induction heating ensures consistent and repeatable results. Once the optimal heating parameters are established, they can be applied consistently to produce uniform results across multiple workpieces. This level of precision and repeatability is crucial in industrial manufacturing to maintain quality standards.

No Surface Contamination: Induction heating does not require direct contact between the heating element and the material being processed. As a result, there is no risk of contamination from the heating element, ensuring the material's purity and integrity remain intact.

Versatility: Induction heating can be applied to a wide range of materials, including metals and some non-metallic materials with high electrical conductivity. This versatility allows it to be used in various industries and applications, such as metalworking, food processing, electronics, automotive, aerospace, and medical treatments.

Compact and Space-Saving: Induction heating systems are generally more compact and space-saving compared to traditional heating methods. The absence of bulky heating elements or furnaces makes it easier to integrate induction heating into existing production lines or to design compact portable systems.

Overall, the advantages of induction heating make it a preferred choice in many industries and applications where efficiency, precision, and safety are essential. While the initial setup cost of an induction heating system may be higher than some traditional heating methods, the long-term benefits in terms of energy savings, improved process control, and reduced maintenance costs often outweigh the initial investment.

6. Use of induction heating in superconducting wire joint

The aim of the induction heating method (Photo 6.1) for jointing MgB_2 superconductor wires is to create a reliable and efficient connection between two separate MgB_2 wires in short time. Jointing or splicing superconducting wires is a critical aspect of their practical applications, especially when longer lengths of wire are required for real-world usage. The induction heating method is employed to achieve a seamless and high-performance joint between the MgB_2 wires.

The induction heating method for jointing MgB_2 superconductor wires is advantageous because it allows for rapid and localized heating, which minimizes the risk of damaging the surrounding areas of the wire. It also enables a high-quality joint with good electrical and mechanical properties, making it suitable for various superconducting applications, including high-field magnets, power transmission cables, and fault current limiters.

Photo 6.1 Joint of MgB_2/Fe wires via our induction heating system.

7. EXPERIMENTAL DETAILS

7.1 Preparation of in-situ MgB2 Powder

Magnesium (pvz) powder with a purity of 99% and a particle size of 74-149 µm and amorphous boron (pvz) powder with a purity of 95-97% and a particle size of less than one µm were used to prepare the primary Mg+2B powder. Based on the stoichiometry of the reactants, we calculated the mass of magnesium and boron required to form 20 g of the Mg+2B mixture; the mass of magnesium is 10.5841 g and the mass of boron is 9.4152 g. The Mg+2B mixture was ground with garnet balls of different sizes (mass ratio 4:1) for 3 hours in the ball mill shown in Photo 7.1. The Mg+2B powder was stored in a bottle covered with parafilm in an argon atmosphere to protect the powder from moisture for as long as possible.

Photo 7.1 Ball milling machine.

7.2 Filling Iron Tube with Mg+2B Powder (PIT)

To make the MgB_2/Fe tube, we used an iron sheath with an outer diameter of 12 mm, an inner diameter of 9 mm, a thickness of 1.5 mm, and a length of 20 cm. Then we close the base of the sheath with aluminum foil, length of 1.5 cm, then we gradually empty the Mg +2B powder into the iron sheath so that the powder reaches the top of the sheath and then close the top with aluminum also with a length of 3 cm, the mass of Mg +2B powder used to fill the iron sheath is 14.503 g. The rest of the unused mixture is 5.4963 g. The PIT used to make the MgB_2/Fe wire is kept in a glove box tightly covered with parafilm (Photo 7.2).

Photo 7.2 Iron sheath with Mg+2B powder inside.

7.3 Wire Making Steps

The superconducting MgB_2/Fe wires were fabricated in situ using the PIT techniques for stoichiometric Mg + 2B powder ratios, and then the iron sheath undergoes a series of drawing and rolling processes to reduce its diameter from 12 mm to 1 mm, resulting in a natural increase in the length of the wire. Photo 7.3 shows the tools and equipment used to produce MgB_2/Fe wires. Table 4.1 shows the drawing steps for the MgB_2/Fe wire.

a) Drawing machine (17 meters)

b) Rolling machine (from 1 mm to 15 mm)

c) Tungsten Carbide Dies (inner diameter from 0.5 mm to 15 mm)

Photo 7.3 In the production of wires, machines such as groove rolling, long wire drawing and dies with different inner diameters are used.

7.4 Closing Both Ends of The Wires

Before heat treating our samples, we need to protect the MgB_2 inside our wires from leaking Mg during heat treatment by sealing the two ends of each sample of our superconducting wires, pressing the two ends of each sample with a pressure of 5 bar using the pressing machine shown in Photo 7.4.

Photo 7.4 Mechanical Press.

7.5 Heat Treatment Process

Heat treatment of MgB_2 nanowires was performed once during wire drawing and several times after drawing. All heat treatment processes were performed using the induction heater shown in Photo 7.5. During the first heat treatment process the MgB_2 wires were heated to 500 °C for 2 minutes per 1 cm. This process facilitates the drawing of the wires and protects them from breakage. Of course, attempts have been made to obtain phase transitions at many temperatures before the above values (from 650 to 1000 °C), but since the optimum superconductor transition temperatures have been observed after 800 °C. After drawing, four samples of 10 cm long MgB_2 wires were heated to temperatures of 800-850-900-950 °C for two minutes under argon flow using an induction heater (Photo 7.6). At this stage, we determined the appropriate temperature based on the R-T measurement results, this temperature was 900 °C. So, in the third heat treatment step, we heat treated three more samples at 900 °C for 5,10, and 20 minutes respectively. The induction heater was chosen as the tool for heat treating of the MgB_2 wire instead of the tube furnace because the samples heat treated with the induction heater seem to have greater flexibility than the wires heat treated with the tube furnace, while maintaining the same superconducting properties in a record time of a few minutes compared to the tube furnace, which take several hours.

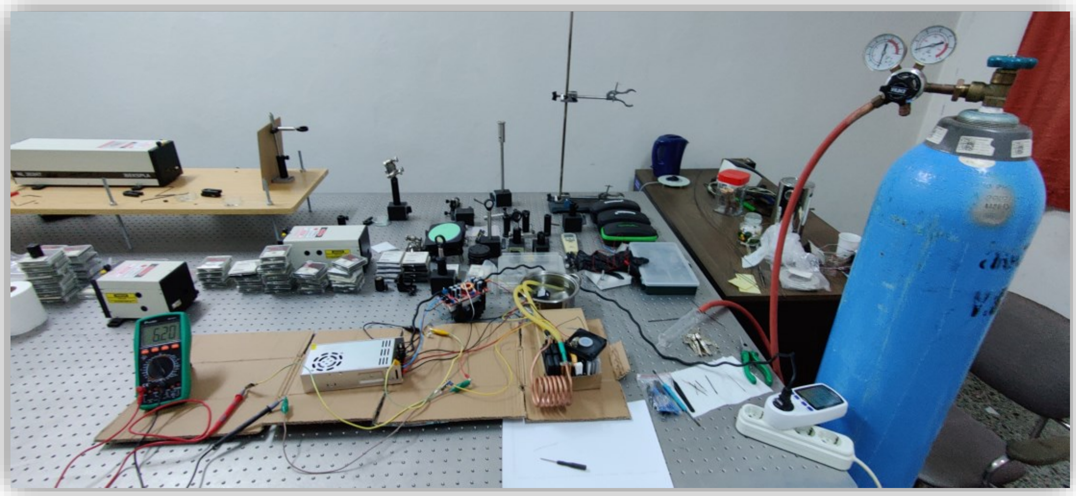

Photo 7.5 1kW induction heating system.

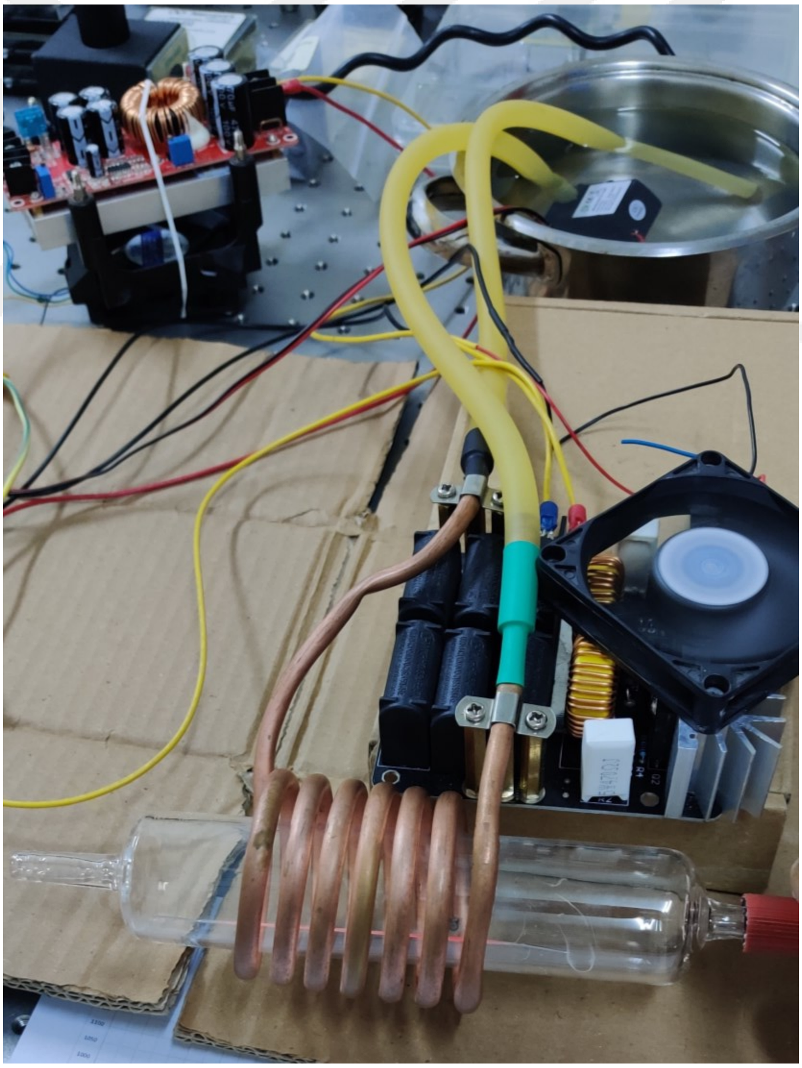

Photo 7.6 MgB_2/Fe wire with a diameter of 1.8 mm, heat treated at a temperature of 900 degrees Celsius for two minutes under argon athmosphere.

7.6 Scanning Electron Microscopy (SEM) Analysis

To observe objects too small for a normal microscope, scientists often use scanning electron microscopy (SEM), in which a beam of electrons is directed at a sample in a vacuum chamber using magnetic lenses. As the electrons interact with the sample's atoms, they reflect beams with unique properties for each atom. This produces a detailed, magnified 3D image in black and white that reveals information about the crystal structure, chemical composition and grain orientation of the surface. In this case, the surface of superconducting MgB_2/Fe wires was analyzed using a scanning electron microscope (JEOL 6390-LV), as shown in Picture 10.7, and SEM images were acquired.

Photo 7.7 SEM device (JEOL 6390-LV).

7.7 Electrical Characterization of The Samples

The four-point probe method is used to determine the electrical transport properties of materials like the electrical conductivity, the resistivity, the hall constant, the charge carrier concentration and the charge carrier mobility. The four-probe technique has been used to measure resistance as a function of temperature (R-T) and current as a function of voltage to determine the temperature at which resistance falls to zero, usually referred to as the critical temperature (T_c), and to determine the critical current density (J_c) values of samples, respectively. The outer probes of the technique are connected directly to the current source, while the inner probes are connected to a voltmeter. The probes are soldered to the MgB_2/Fe wire samples with a mixture of 60 percent tin and 40 percent lead. Four samples were simultaneously attached to the sample holder of the helium-gas contact cryostat system (Picture 10.8) using GE varnish, and the other ends of the soldered copper wires were soldered to the measurement tips. The R-T measurement was performed by applying 100 mA current to each sample, with a heating rate of 2°/min. in the temperature range of 10-50 K. I-V measurements of the samples were made in the same system by applying a current in 0.05 A steps ranging from 0-1 A, while the temperature was fixed at 25 K. The value for the critical current density (J_c) was determined by measuring the voltage-current relationship, using 1 V/cm as the criterion. The cryostat system can be operated with a maximum DC current of 1 A and a maximum magnetic field of 7 T.

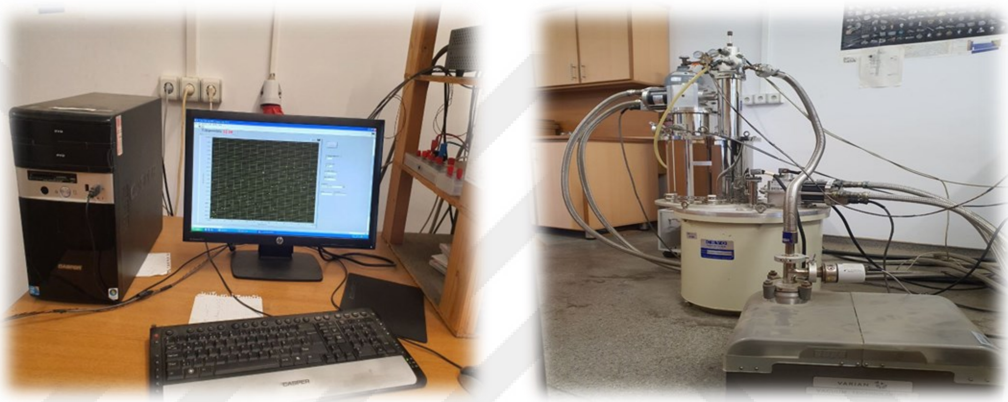

Photo 7.8 7 T 2.2 K cryostat system for the characterization of superconducting properties of the samples.

8. RESULTS AND DISCUSSION

In this study, in-situ MgB_2/Fe wires were fabricated by the PIT method and annealed by induction heating. Electrical (R-T and I-V) and structural characterizations (SEM and EDS (Energy Dispersive Spectroscopy)) of the obtained samples were performed. The following subsections contain the results and comments.

8.1 Magnetoresistivity Measurements

In Figures 8.1 to 8.10, the resistivity behavior of the iron-sheathed MgB_2 material prepared by the in situ PIT method was investigated under the magnetic field (0, 1, 3, and 5 T) of samples treated with induction heating (under argon flow) at 900 ℃ for certain periods of time. Samples about 2-2.5 cm long were cut from the center of our wires, which were originally 10 cm long and had an outer diameter of 1.8 mm, with both ends closed. Insulated copper wires were soldered to these samples using the four-point contact method. For the resistivity-temperature measurements, the samples were placed in the sample holder of the helium gas contact cryostat system. For the R-T measurements, a DC current of 100 mA was applied from the two outer ends of the four-point contact. Then, the distance between the voltage terminals of the samples and the sample diameters were measured with a caliper and the resistance temperature curves were determined by inserting them into the resistivity formula.

All results obtained from the resistivity vs. temperature curves of the samples are shown in Table 8.1. When comparing the samples heat treated at different temperatures for the same time, the highest critical transition temperature (37.6 K) was observed for the sample at 900 °C for 10 minutes (sample G) under self magnetic field (0T). However when comparing the resistivity values of these samples the one with the lowest resistivity is at 900 °C for 2 minutes (4.8 $\mu\Omega\cdot$cm). Of course, it is not possible to determine the best with the critical temperature alone, but considering these values, the results of heat treatment at 900 °C for 1, 5 and 10 minutes were compared with the results of heat treatment in 2 minutes. When samples A, C, E and G, heat-treated at the same temperature for different lengths of time, were compared with each other, the highest critical transition temperature was found for samples C and G.

Examining the magnetoresistance measurements in Figures 8.1 through 8.10, it can be seen that as the magnetic field increases, the critical transition temperatures decrease as expected. When comparing all samples, it was found that there are slight differences in the critical transition temperatures that can be considered a margin for experimental error. But when comparing samples F and H to all samples, it was concluded that aluminum that we used for joint was deformed by annealing and this is because we observed huge transition for these samples.

Table 8.1 Critical temperature values of the samples A, B, C, D, E, F, G, and H.

Samples	Heat treatment temperature(°C)	Induction heating time (minute)	Critical temperature T_c (K), (0T)	T_c^{onset} (K), (0T)	T_c^{offset} (K), (0T)	$\Delta T = T_c^{onset} - T_c^{offset}$ (K)
A	900	1	35.5	33.9	37.5	4.6
B	900 joint	1	35.4	33.3	38.4	5.1
C	900	2	37.4	36.9	38.7	1.8
D	900 joint	2	36.2	34.2	38.5	4.3
E	900	5	36.8	36.0	38.7	1.9
F	900 joint	5	32.1	25.8	38.5	12.7
G	900	10	37.6	36.9	38.7	1.8
H	900 joint	10	30.9	24.4	38.5	14.1

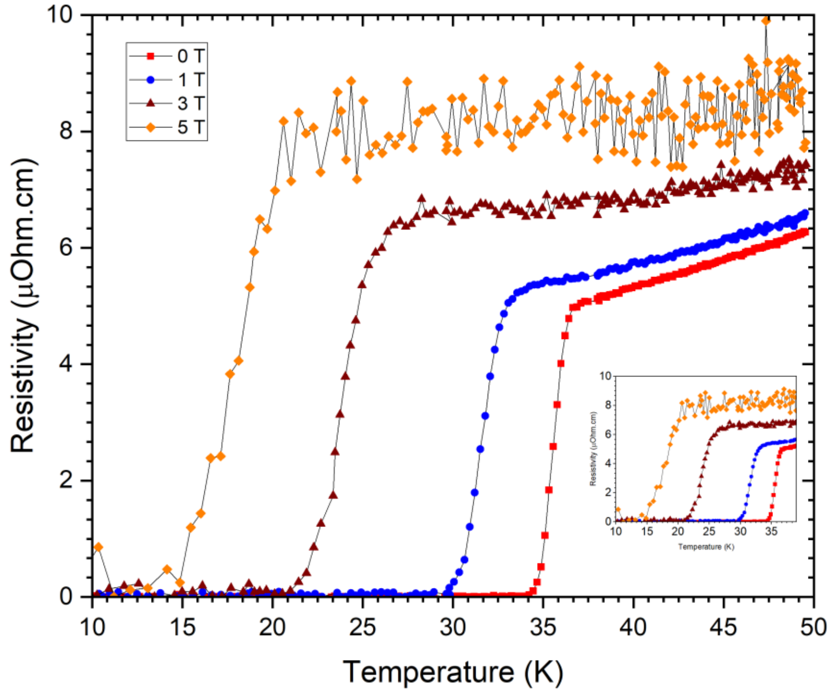

Figure 8.1 Magnetoresistivity measurement of sample A.

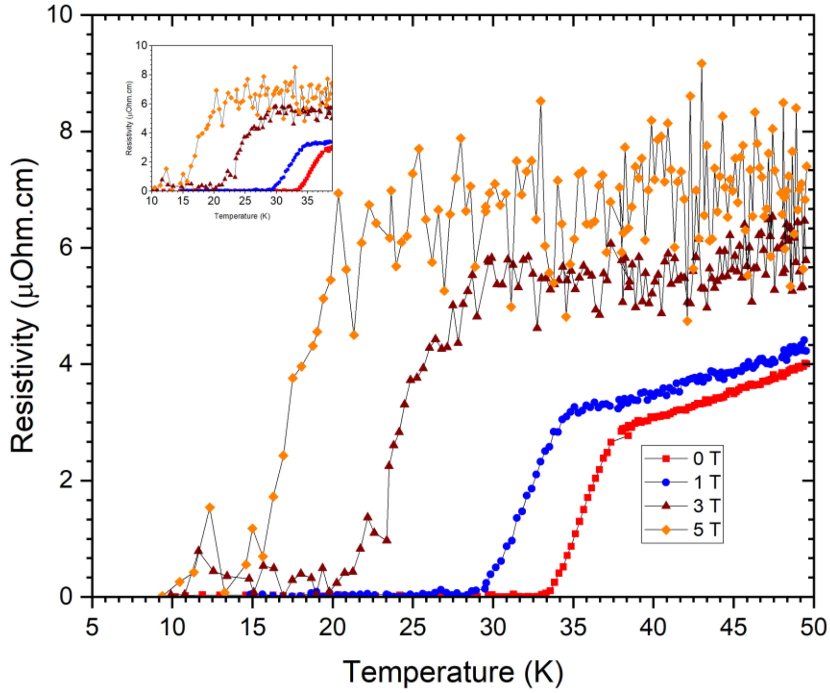

Figure 8.2 Magnetoresistivity measurement of sample B.

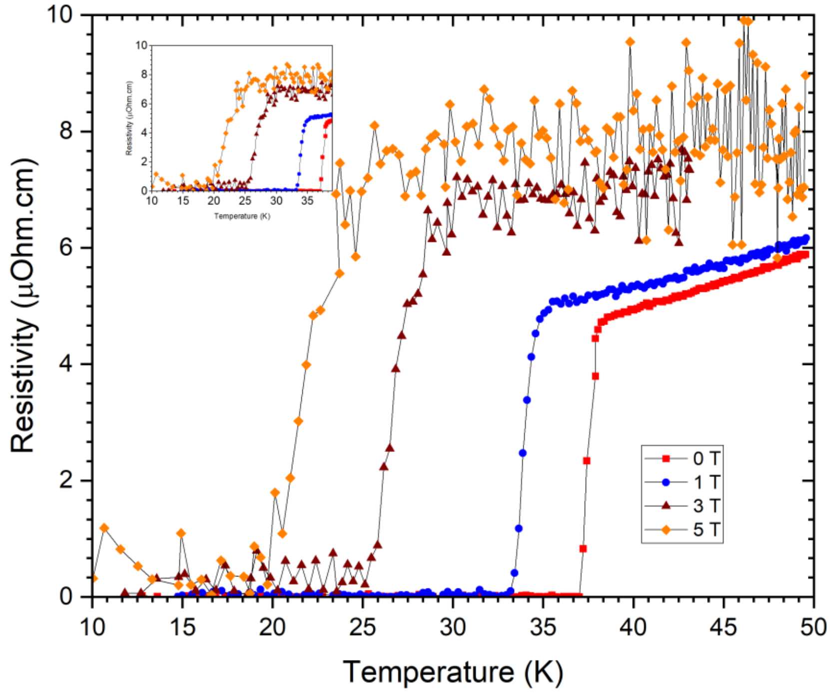

Figure 8.3 Magnetoresistivity measurement of sample C.

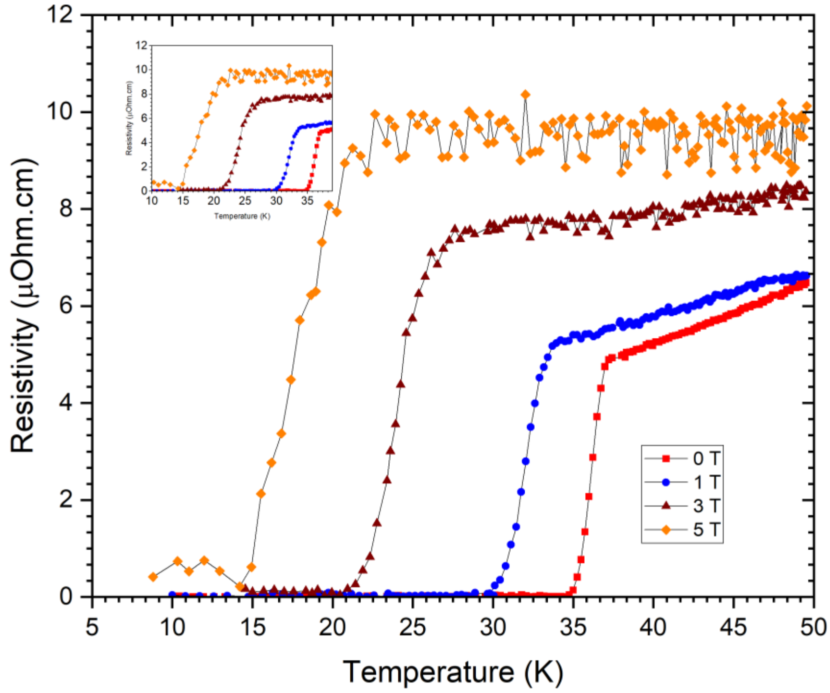

Figure 8.4 Magnetoresistivity measurement of sample D.

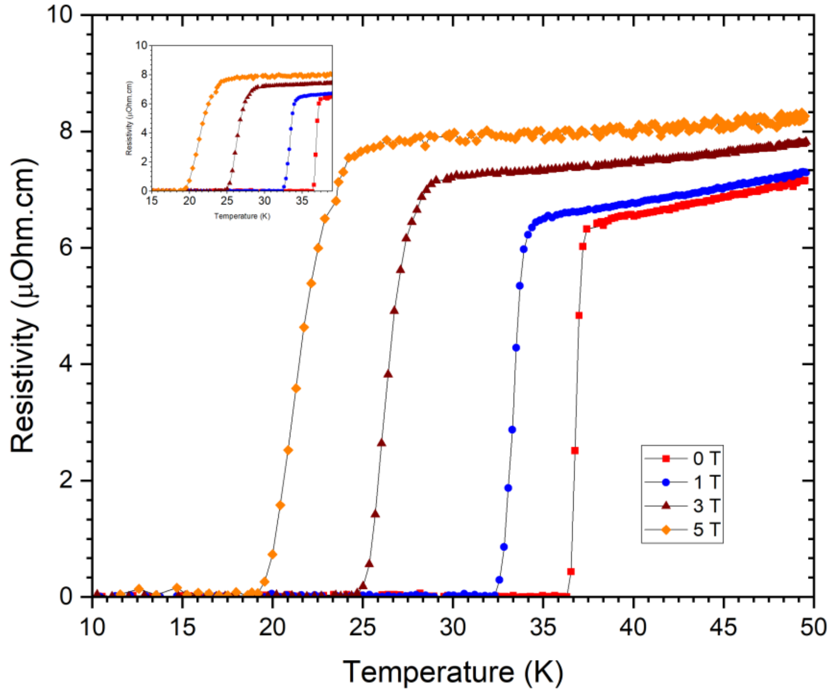

Figure 8.5 Magnetoresistivity measurement of sample E.

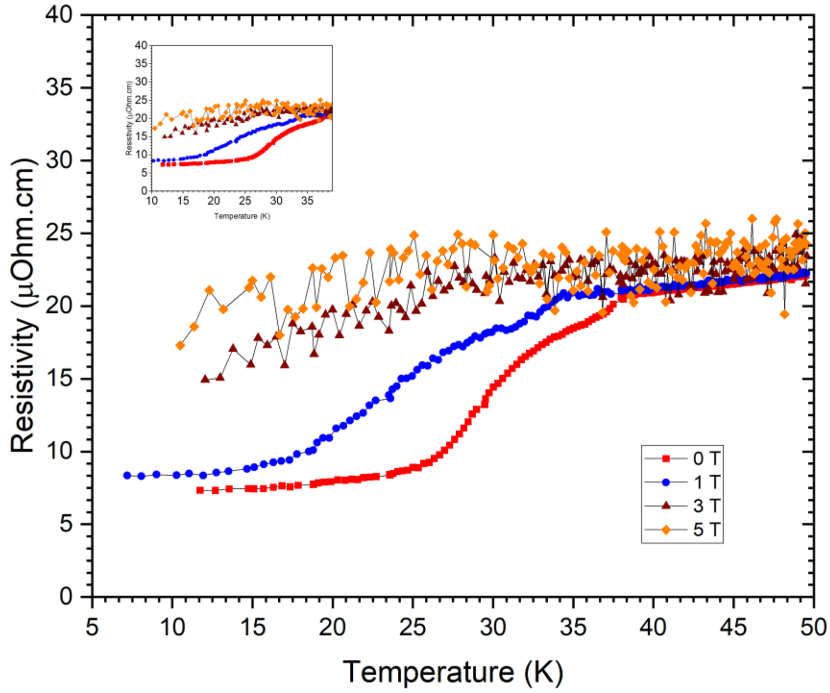

Figure 8.6 Magnetoresistivity measurement of sample F.

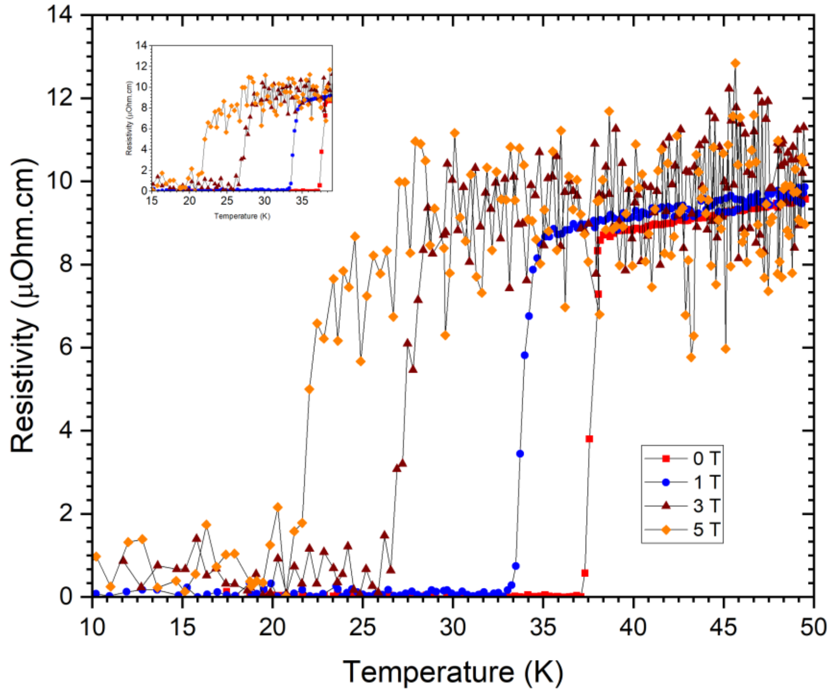

Figure 8.7 Magnetoresistivity measurement of sample G.

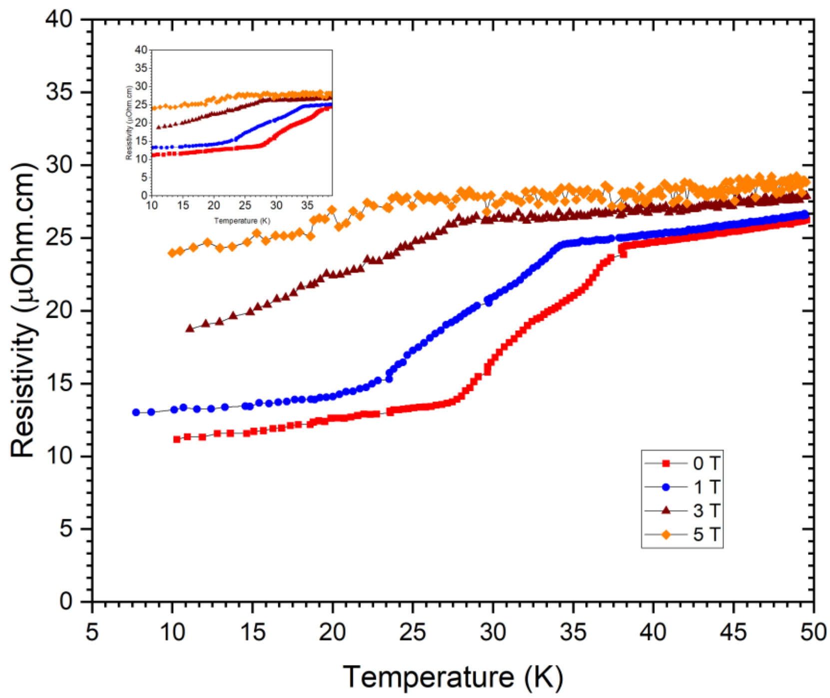

Figure 8.8 Magnetoresistivity measurement of sample H.

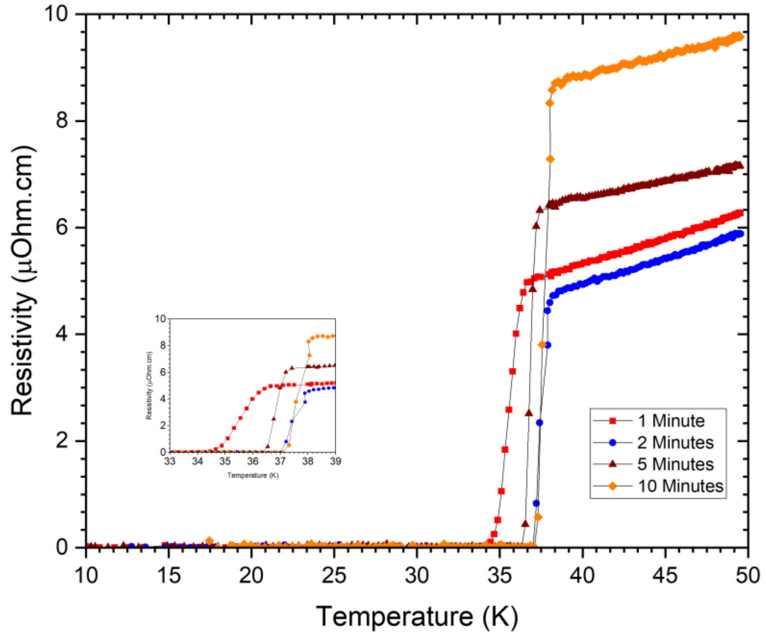

Figure 8.9 Magnetoresistivty measurement comparison of samples A, C, E, and G in self-field.

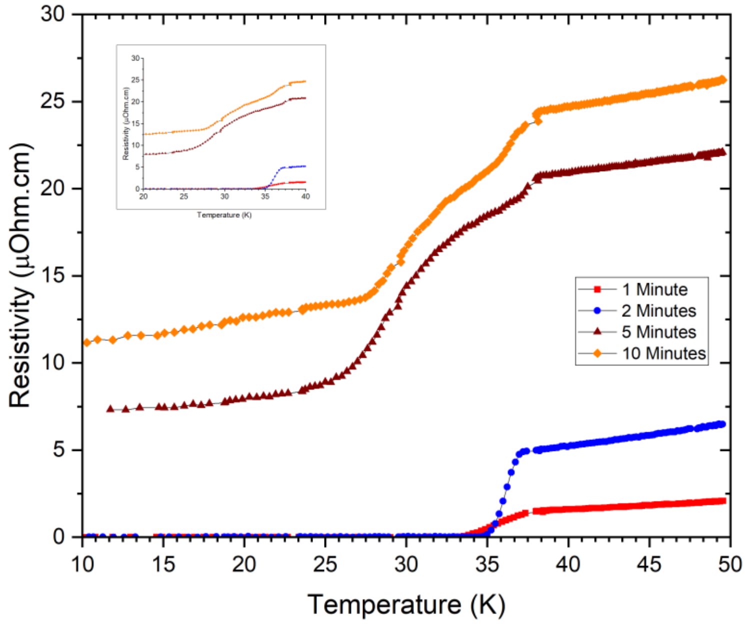

Figure 8.10 Magnetoresistivity measurement comparison of samples B, D, F, and H in self field.

8.2 Current-Voltage (I-V) Measurements

Under normal conditions, making I-V measurements with high-current supplies in the liquid helium environment provides more advantageous and reliable results. However, the increasing cost of liquid helium and the impracticalities lead us to the current possibilities. The power source connected to our cryostat system can supply a maximum of 1 A of current. For this reason, we make our measurements by setting our temperature controller to a value as close as possible to the critical temperature. Based on our previous experience, we set the temperature controller to 25 K. After waiting about 1 hour for this temperature value to settle, we started making I-V measurements under the magnetic field. The reason we apply a magnetic field is so that we can see the transition from the superconductor to the normal state. Otherwise, since the sample carries a very high current, it is not possible to observe the transition from the superconductor to the normal conductor state. In our cryostat system, a maximum magnetic field of 7T can be applied. The applied magnetic field is perpendicular to the longitudinal section of the sample. The measurement results are shown in from Figure 8.12 to Figure 8.19 for all samples. The data from these measurements are shown in Table 8.2. The values given in the table for the engineering critical current density were calculated from the I-V curves using the 1 μV/cm criterion and taking into account the sample sizes.

As you can see from Table 8.2, all samples have different engineering critical current densities. Note that for samples F and G, "Metallic behavior" is indicated. This is because the joint metal was deformed by annealing. In our future studies, we plan to replace joint metal with one resistant to high temperatures.

Comparing the critical current density values calculated from the I-V measurements of the samples annealed at 900 °C with different time intervals, we can say that a minimum current carrying capacity of 4 A/cm^2 at 2 T and above was obtained in all samples except F and H.

Table 8.2 Engineering critical current densities of the samples.

sample	**Temperature(°C)**	**Time(minutes)**	**J_e (A/cm^2) (at 25 K)**
A	900	1	9.83 (2 T)
B	900	1	5.18 (2.5 T)
C	900	2	2.94 (2.5 T)
D	900	2	4.18 (2 T)
E	900	5	8.84 (3 T)
F	900	5	Metallic behavior
G	900	10	37.35 (3 T), 0.98 (4 T)
H	900	10	Metallic behavior

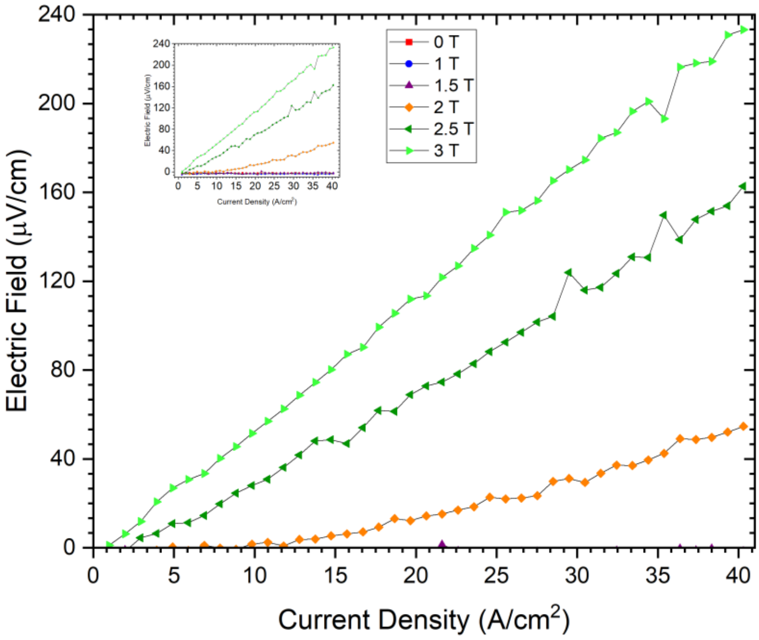

Figure 8.11 Measurement of Electric field versus Current Density of the sample A at different magnetic fields from 0 to 3 T at 25 K.

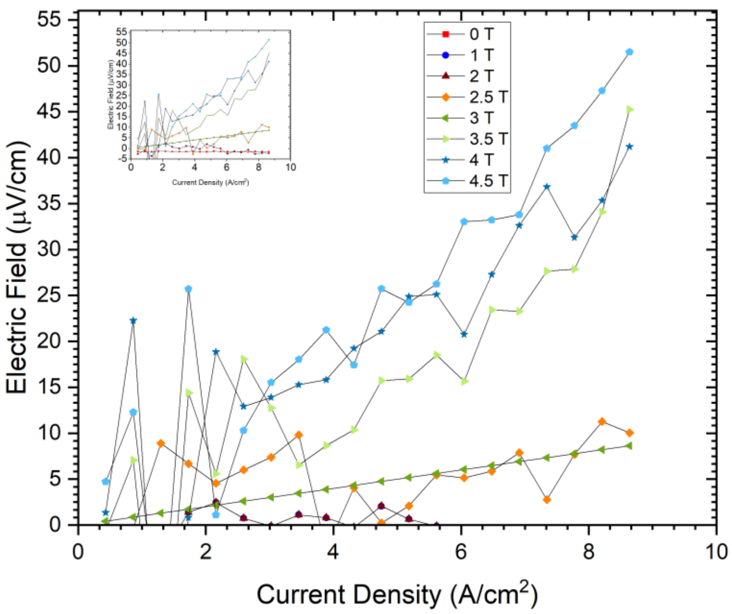

Figure 8.12 Measurement of Electric field versus Current Density of the sample B at different magnetic fields from 0 to 3 T at 25 K.

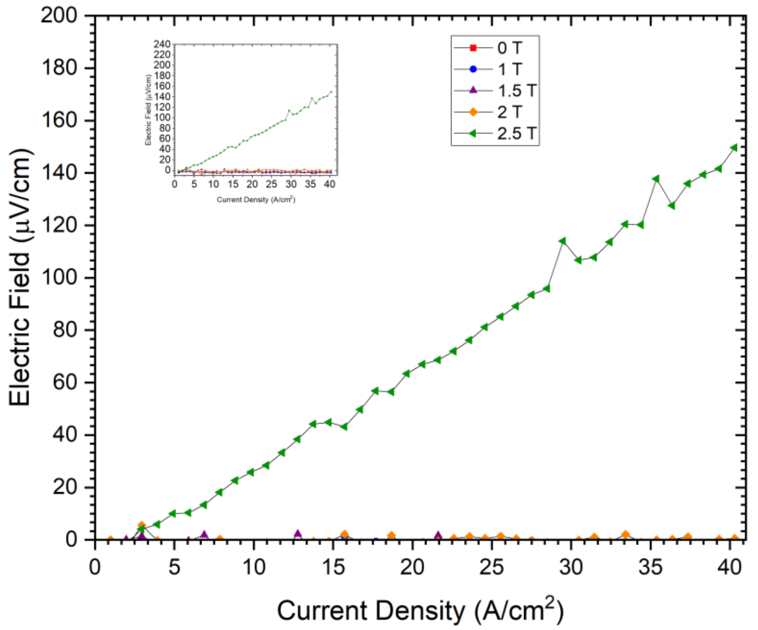

Figure 8.13 Measurement of Electric field versus Current Density of the sample C at different magnetic fields from 0 to 3 T at 25 K.

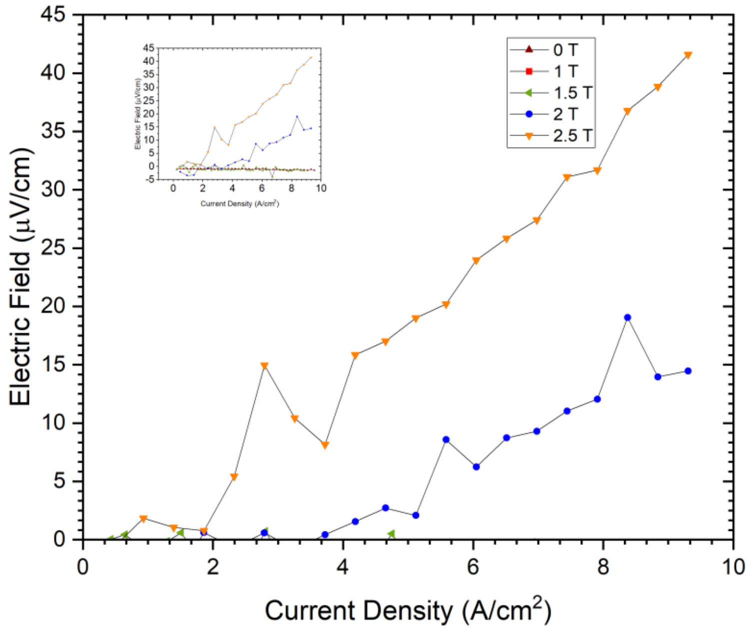

Figure 8.14 Measurement of Electric field versus Current Density of the sample D at different magnetic fields from 0 to 3 T at 25 K.

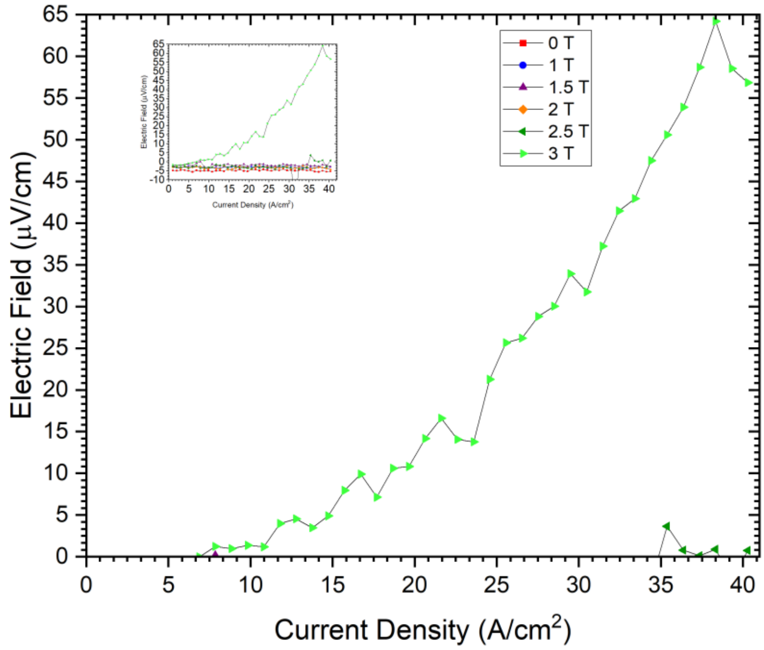

Figure 8.15 Measurement of Electric field versus Current Density of the sample E at different magnetic fields from 0 to 3 T at 25 K.

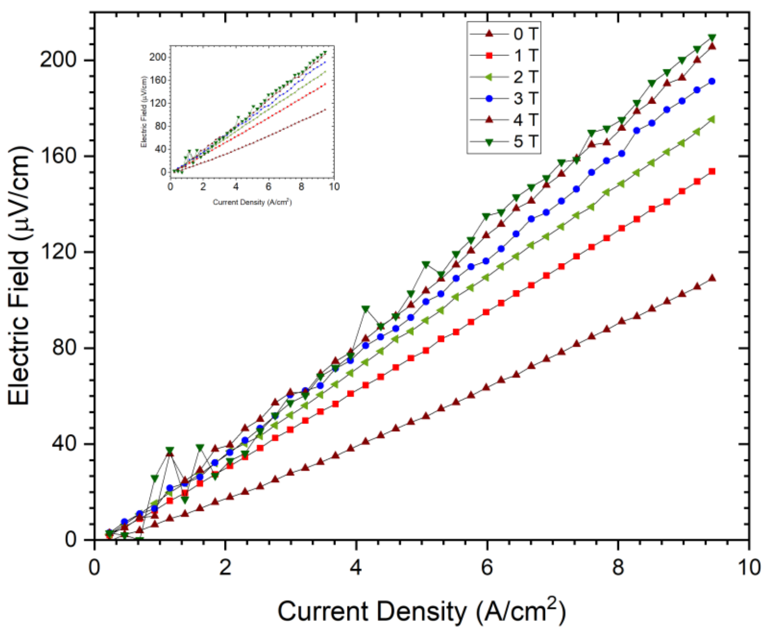

Figure 8.16 Measurement of Electric field versus Current Density of the sample F at different magnetic fields from 0 to 3 T at 25 K.

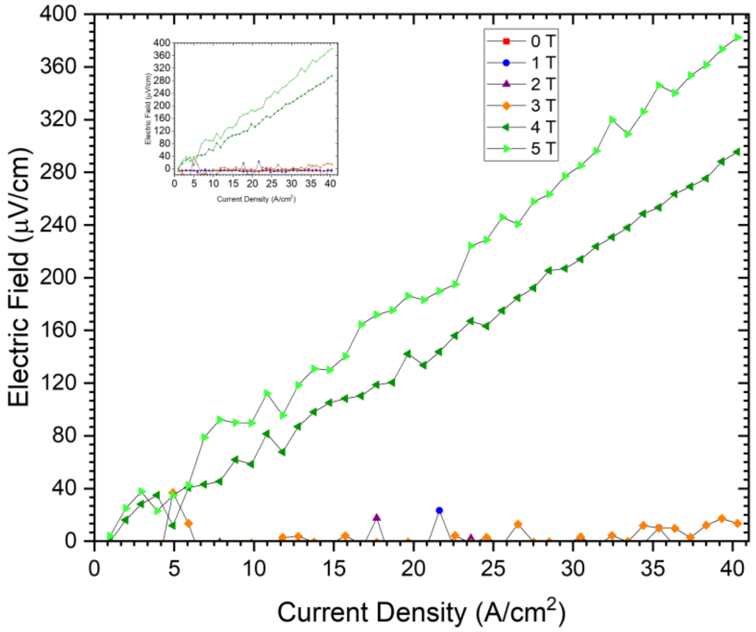

Figure 8.17 Measurement of Electric field versus Current Density of the sample G at different magnetic fields from 0 to 3 T at 25 K.

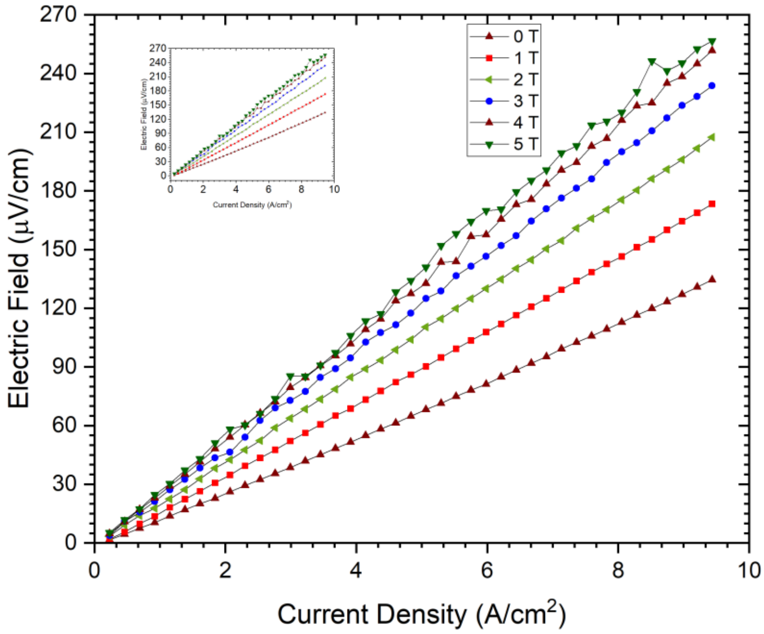

Figure 8.18 Measurement of Electric field versus Current Density of the sample H at different magnetic fields from 0 to 3 T at 25 K.

8.3 Scanning Electron Microscope (SEM) Analysis

The surface analyzes of the samples were performed using JEOL brand scanning electron microscope, model 6390- LV, in Bolu Abant İzzet Baysal University Faculty of Arts and Sciences. Detailed SEM images for different samples in different scales from Figure 8.20 to 8.25. Figures contain images of cross-sectional surfaces of reacted samples. These images were taken after the surfaces of the samples were sanded. As you can see, the wires have a perfectly regular circular structure.

Figures 8.20 through 8.25 show SEM images of the samples annealed at 900 °C for various times, taken at 100, 1000, 3000 and 5000 magnifications. In general, the samples contain voids, pores, and cracks. However, as can be seen from the resistivity versus temperature curves and the I-V results, it is clear that these structures do not prevent the formation of superconductivity and current carrying of the samples. However, as we know from the literature and our experience, the denser the core of a sample, the higher its current carrying capacity. When we examined the picture of each sample showing the transition from the core region to the iron sheath, no iron oxide-like structures were found. Therefore, we can say that induction heating, which we performed in an argon atmosphere, works very well at this point. However, when the joint is taken into account, especially for the aluminum purchased from the hardware store that we used, annealing processes after 5 minutes caused deformation in the aluminum, which deteriorated its superconductivity properties.

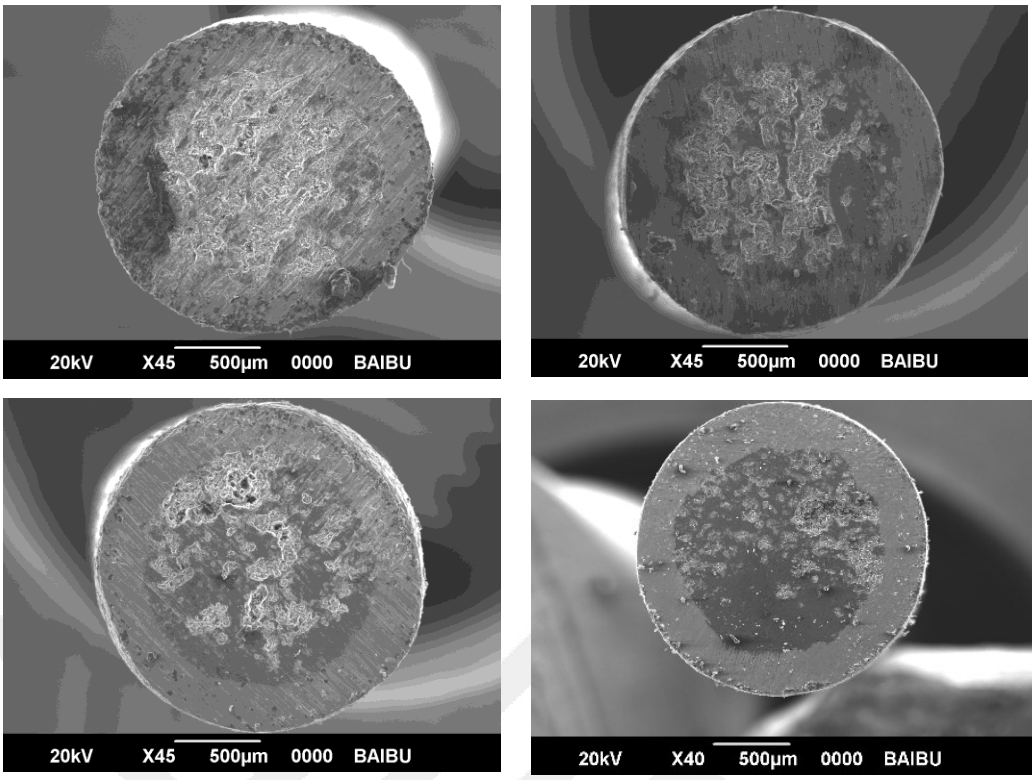

Figure 8.19 Cross-sectional SEM pictures of the samples, A, C, E, and G.

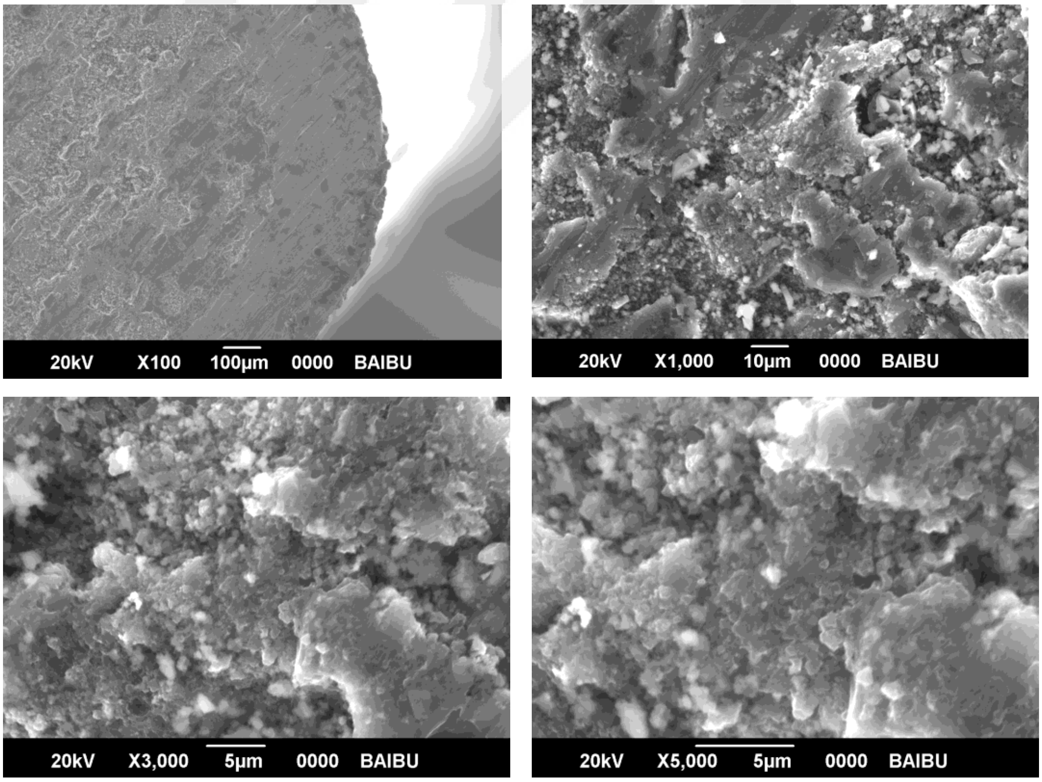

Figure 8.20 SEM images of sample A at different magnetizations from 100 to 5000.

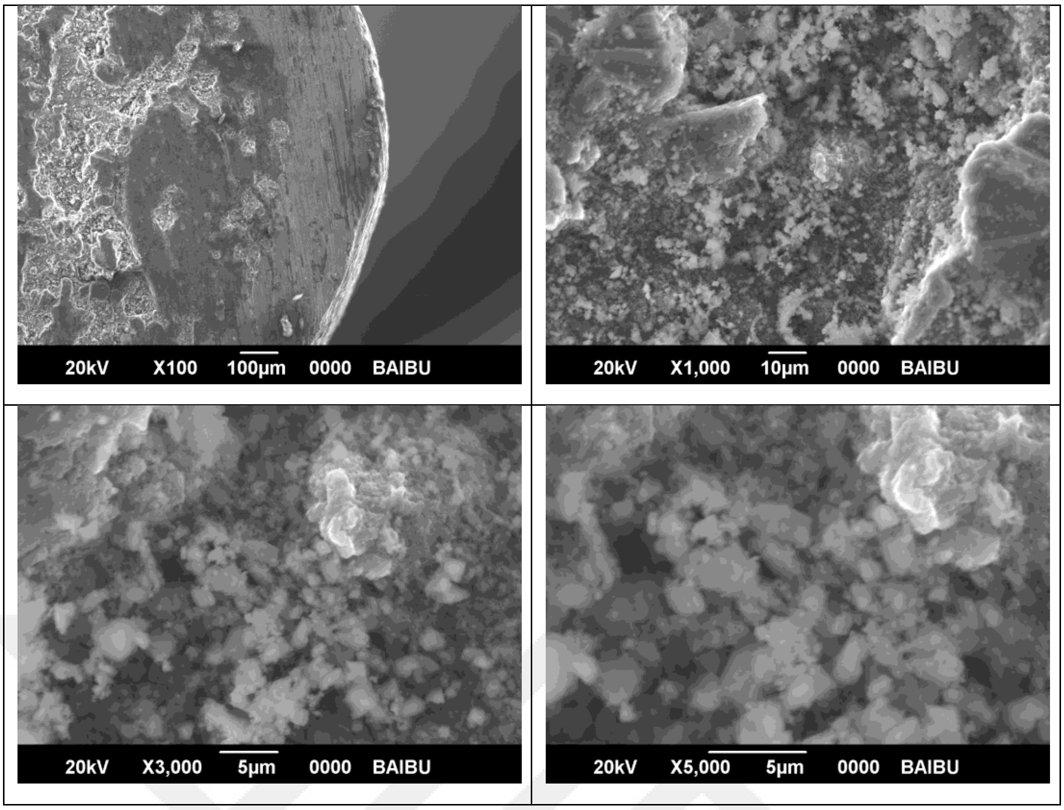

Figure 8.21 SEM images of sample C at different magnetizations from 100 to 5000.

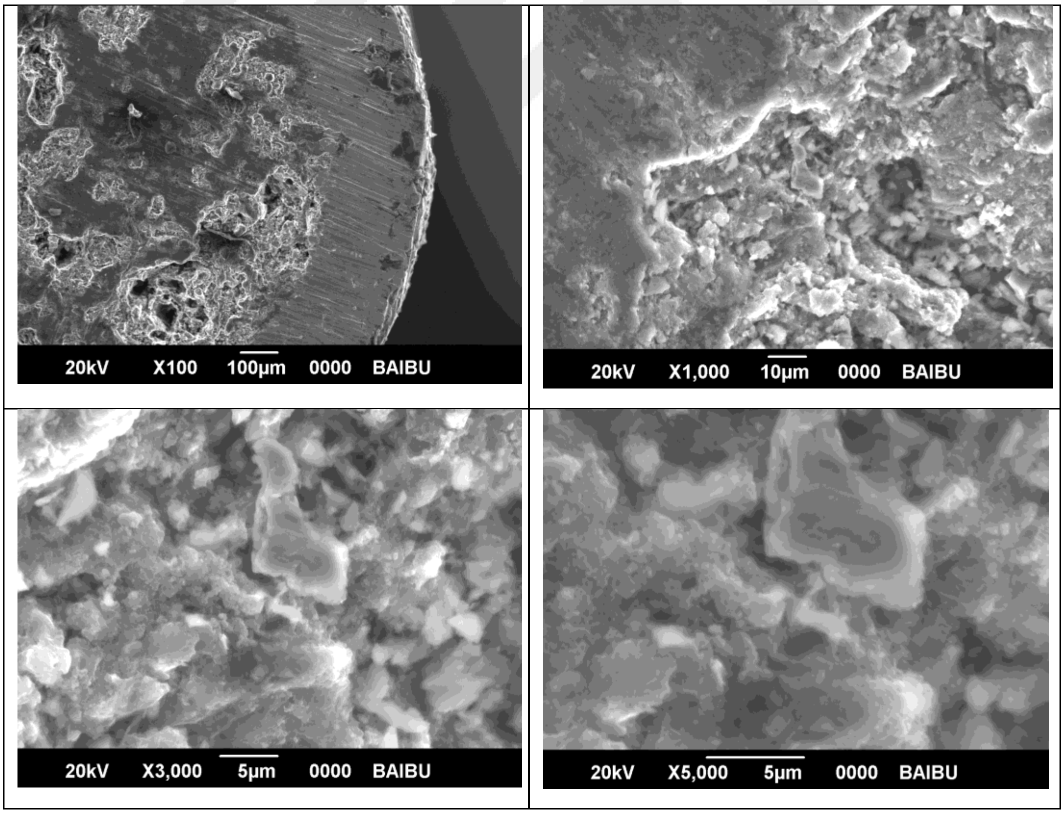

Figure 8.22 SEM images of sample E at different magnetizations from 100 to 5000.

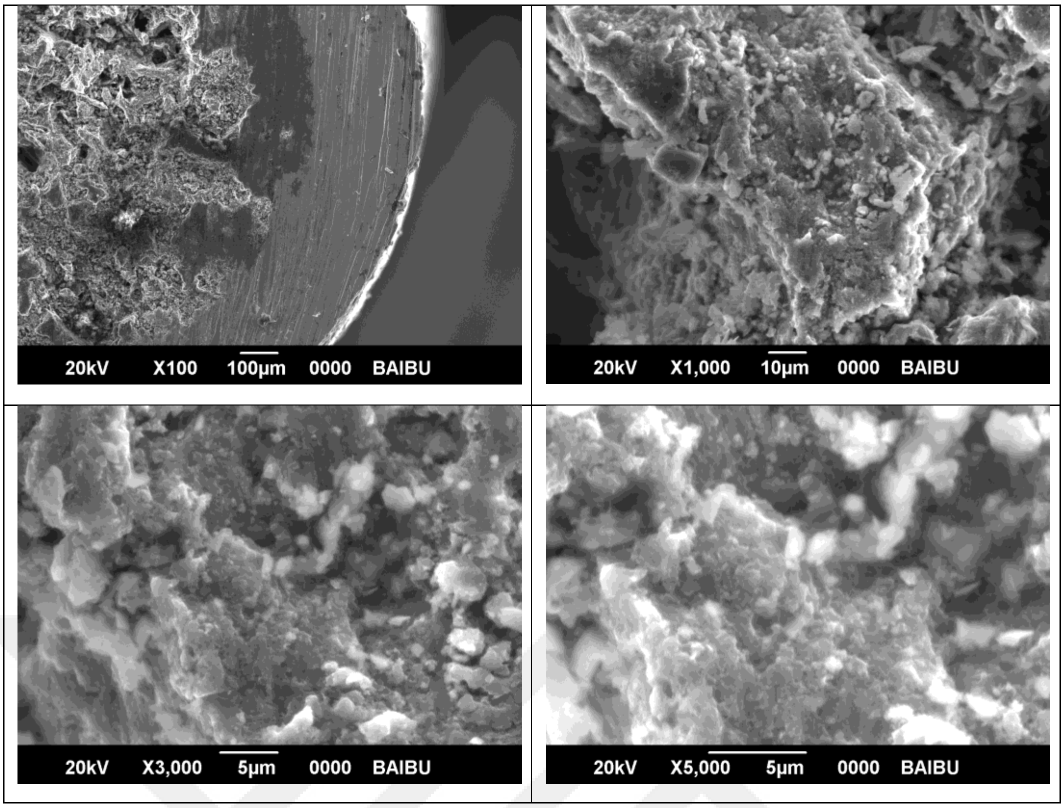

Figure 8.23 SEM images of sample G at magnetizations from 100 to 5000.

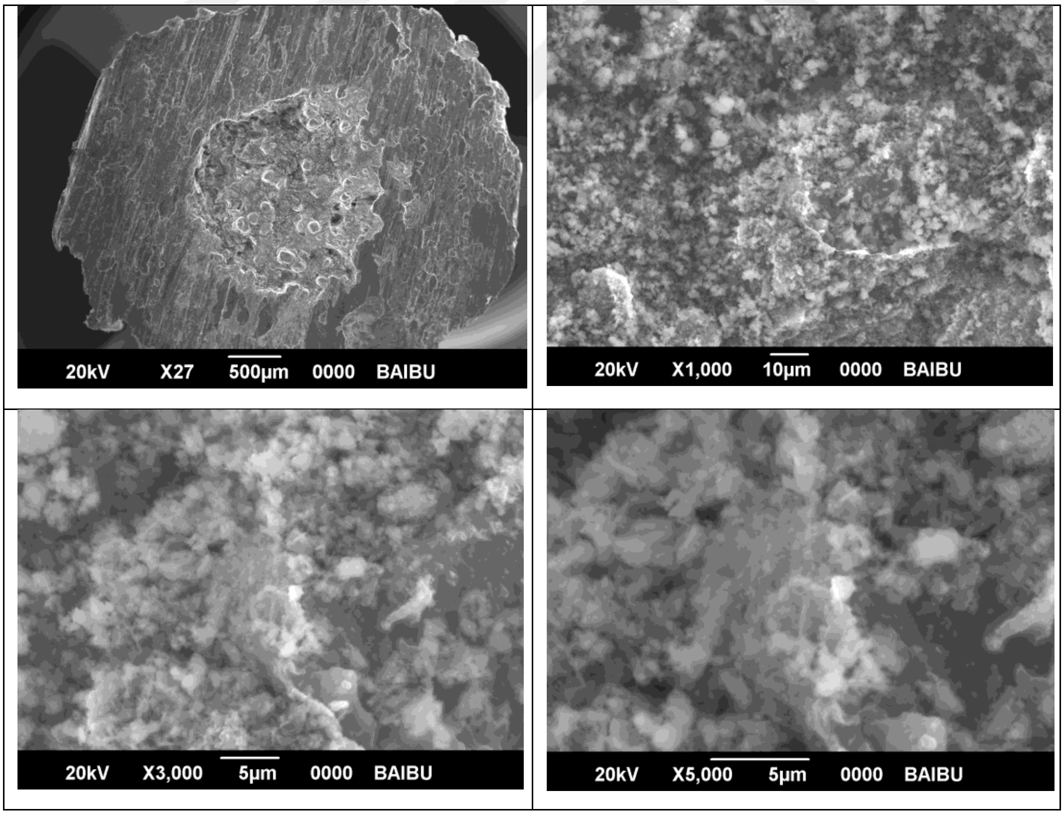

Figure 8.24 SEM pictures of sample H at magnetizations from 100 to 5000.

8.4 Energy Dispersive Spectroscopy (EDS) Analysis

EDS is popular microanalytical technique that is used to identify and quantify the elements present in a sample. EDS can be used to create elemental maps of samples via working alongside a scanning electron microscope (SEM). Figures 8.26 to 8.29 show the elemental maps obtained from the EDS scan of samples A, C, E and G. Figure 8.30 shows the elemental analysis of the cross-section of sample H. These maps give us an idea of the distribution of elemental densities in the regions we analyzed. In these maps (from Figures 8.26 to 8.29), boron is colored red, iron blue and magnesium green. On the other hand, the colors in the map of sample H at Figure 8.30 are defined as blue for aluminum, green for magnesium and red for boron. Table 8.3 shows the percentage distribution of the elements in the samples. Depending on which part of the sample you analyze, changes in the percentages of the elements can be observed. All we can say here is this: The B:Mg ratio in the area where the G sample, 900 °C and 10 minutes, was analyzed with the best current carrying capacity is 1:2. In all other samples it varies greatly from this.

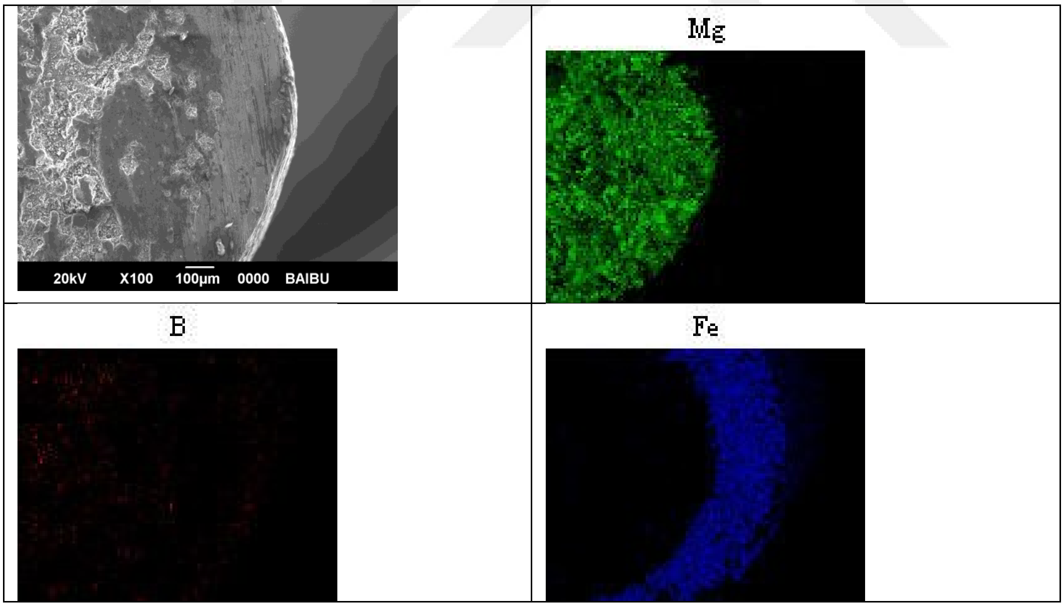

Figure 8.25 Elemental maps of sample A.

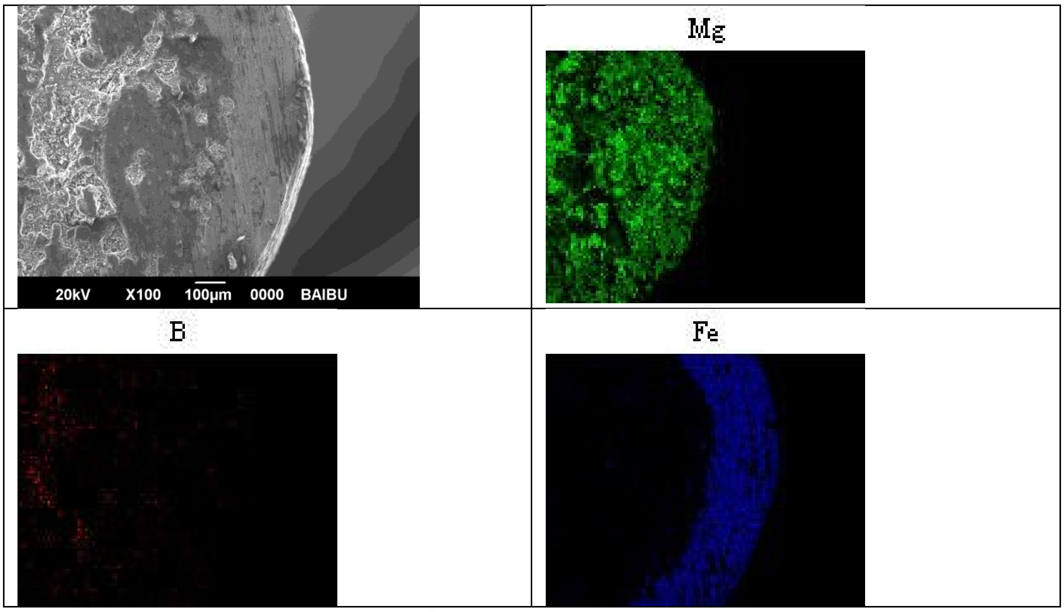

Figure 8.26 Elemental maps of sample C.

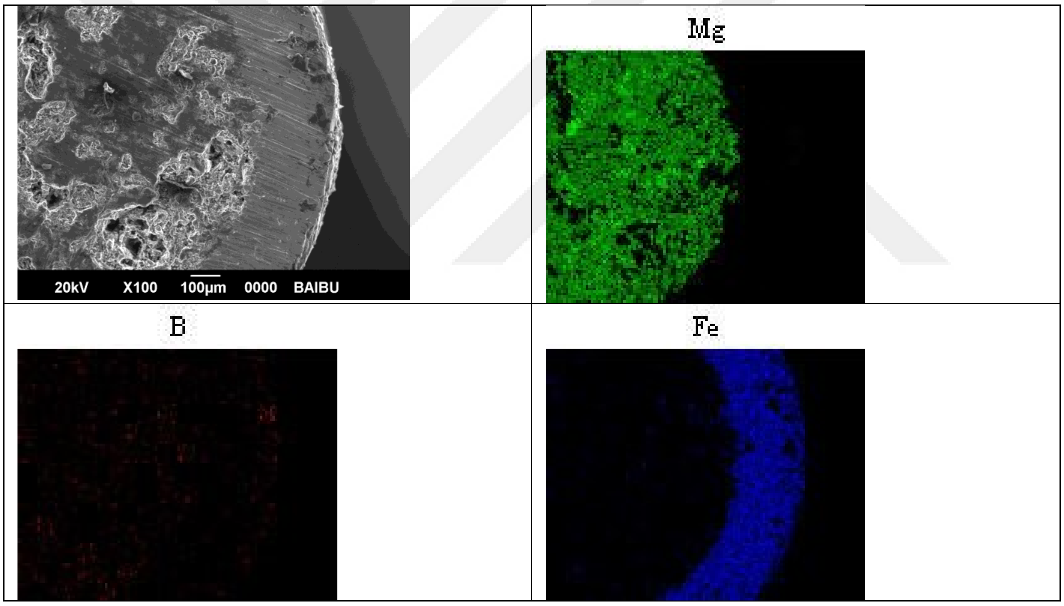

Figure 8.27 Elemental maps of sample E.

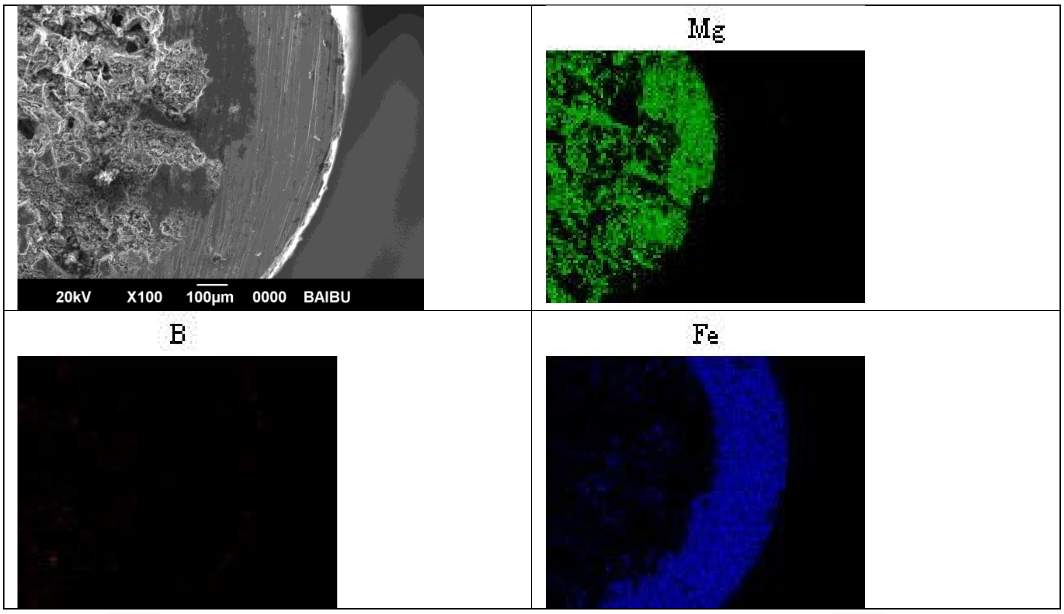

Figure 8.28 Elemental maps of sample G.

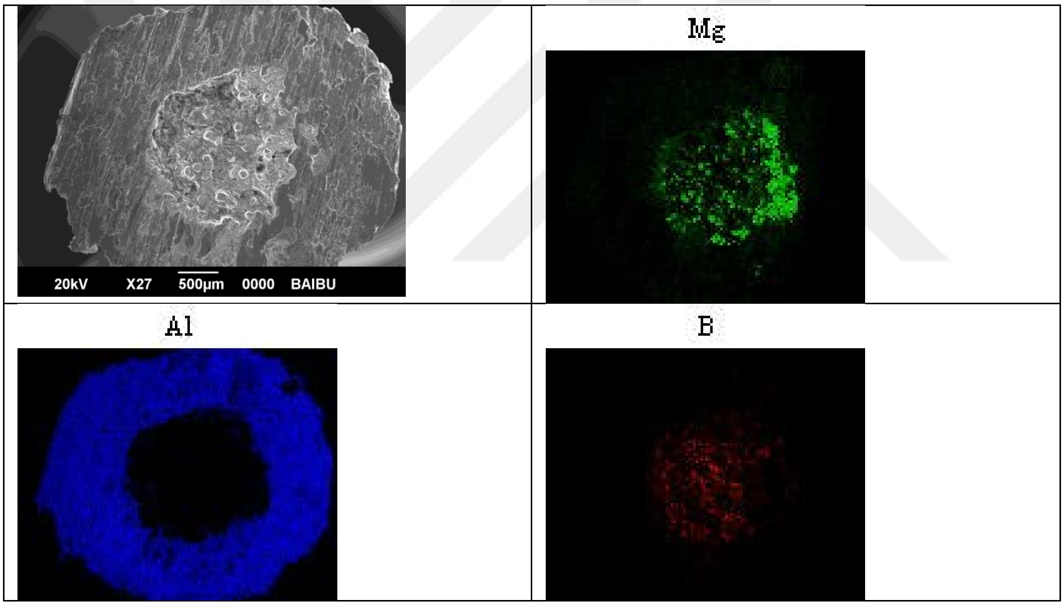

Figure 8.29 Elemental maps of sample H.

Table 8.3 Element distributions of the samples in percent by weight.

Samples	*Element*	*Type*	*Line*	*Concentration (wt. %)*
A	**B**	Calc	K_α	56.070
	Mg	Calc	K_α	34.304
	Fe	Calc	K_α	9.626
			Total	**100**
C	**B**	Calc	K_α	43.392
	Mg	Calc	K_α	42.274
	Fe	Calc	K_α	14.334
			Total	**100**
E	**B**	Calc	K_α	9.109
	Mg	Calc	K_α	71.096
	Fe	Calc	K_α	19.796
			Total	**100**
G	**B**	Calc	K_α	21.207
	Mg	Calc	K_α	40.832
	Fe	Calc	K_α	37.961
			Total	**100**
H	**B**	Calc	K_α	30.424
	Mg	Calc	K_α	8.670
	A	Calc	K_α	60.906
			Total	**100**

9. CONCLUSION

In planning this study, we started from the idea of finding an alternative solution to the difficulties of producing superconducting wires of long- length. In response to many alternative joint applications, we designed a joint solution using our newly developed induction heating method. In this method, we took one of the wires with a diameter of 1.8 mm, which we had cut into 10 cm length and divided into two parts, and used aluminum tube pieces we bought from the hardware store as intermediate connectors. First, we inserted one end of the wire into the aluminum tube and pressed it together with the hydraulic hand press we had bought, creating a gap at the other end of the tube. We put Mg+B powder and some more Mg powder on the other free end and placed the other piece of wire and compressed this wire with the hydraulic hand press. We sealed both ends of the joined wires we had obtained and the other sample wires we had previously adjusted with a mechanical press and performed heat treatment for 1, 2, 5 and 10 minutes with the induction heater we had developed and performed magnetoresistance, I-V characteristics and SEM and EDS analyzes.

After the annealing temperatures we conducted, the deformation that occurred especially in the aluminum parts of the jointed samples annealed for 5 and 10 minutes had a negative effect on the magnetoresistive and I-V measurement results. Therefore, metallic behavior was observed in the I-V results of the F and H samples and large superconductivity transitions of 12.7 K and 14.1 K were obtained in the R-T measurements (under magnetic field). The expected results were obtained for the R-T and I-V characteristics of the other A, B, C, D, E and G samples. For example, the T_c values of samples A and B are very close to each other and are 33.9 K and 33.3 K, respectively. The critical current densities determined from the I-V results at 25 K are 9.83 A/cm^2 (at 2 T) and 5.18 A/cm^2 (at 2.5 T). The T_c values of samples C and D are 37.4 K and 36.2 K, respectively, and the critical current densities determined from the I-V results at 25 K are 2.94 A/cm^2 (at 2.5 T) and 4.18 A/cm^2 (at 2 T), respectively. Finally, the T_c values of samples E and G are 36.8 and 37.6 K, and the critical current density values at 25 K are 8.84 A/cm^2 (at 3 T) and 37.35 A/cm^2 (at 3 T)/0.98 A/cm^2 (at 4 T). The evaluation of these measurement results shows that superconducting transition temperatures of 35 K and above are achieved for all samples except for samples F and H. At the critical current densities, which were calculated as a result of the I-V tests at 25 K, a minimum current carrying capacity of 4.18 A/cm^2 is achieved in magnetic fields of 2 T and above.

When looking at the SEM analyzes, it was found that the voids in the E and G samples increased in proportion to the annealing time compared to the A and C samples, with the adhesion between the particles being more pronounced in the E and G samples. A similar structure was also found in the H sample, the intersection of which was examined. Although the EDS analyzes did not provide a clear result, they gave us information about the percentage weights of boron, magnesium, iron and aluminum.

The results obtained with this study and the studies planned for the future can be summarized as follows:

1- This study has proven that superconducting wires can be joined by induction heating after annealing for 1 minute.
2- The joining material used is a material with an unknown percentage purchased from a hardware store. Therefore, repeating this process with a different metal with a known percentage and high temperature resistance will lead to serious results.
3- Also, after changing the joint material, detailed studies on different annealing times may be required.
4- The designed induction heating system has a fixed frequency of 100 kHz. If it is adapted to other frequencies in future studies, it will be possible to induce other metal materials.

REFERENCES

Akdoğan, M., Yetiş, H., Gajda, D., Karaboğa, F., Rogacki, K., Morawski, A., & Belenli, İ. (2017). Use of amorphous boron and amorphous nano boron powder mixture in fabrication of long in-situ MgB2/Fe wires. *Journal of Alloys and Compounds*, *702*, 399–403. https://doi.org/10.1016/j.jallcom.2017.01.142

Akdoğan, M., Yetiş, H., Gajda, D., Karaboğa, F., Ülgen, A. T., Demirtürk, E., & Belenli, İ. (2015). Effect of the initial filling density on the critical current of in-situ Fe/MgB2 wires. *Journal of Alloys and Compounds*, *649*, 1007–1010. https://doi.org/10.1016/j.jallcom.2015.07.165

Aldica, G., Burdusel, M., Popa, S., Pasuk, I., Ionescu, A. M., Kuncser, A., & Badica, P. (2018). Ex Situ Spark Plasma Sintering of Short Powder-in-Tube MgB2 Tapes with Open and Closed Ends. *Journal of Superconductivity and Novel Magnetism*, *31*(11), 3423–3432. https://doi.org/10.1007/s10948-018-4616-9

Ballarino, A., Bruzek, C. E., Dittmar, N., Giannelli, S., Goldacker, W., Grasso, G., Grilli, F., Haberstroh, C., Hole, S., Lesur, F., Marian, A., Martinez-Val, J. M., Martini, L., Rubbia, C., Salmieri, D., Schmidt, F., & Tropeano, M. (2016). The BEST PATHS Project on MgB2 Superconducting Cables for Very High Power Transmission. *IEEE Transactions on Applied Superconductivity*, *26*(3). https://doi.org/10.1109/TASC.2016.2545116

Canfield, P. C., Finnemore, D. K., Bud'ko, S. L., Ostenson, J. E., Lapertot, G., Cunningham, C. E., & Petrovic, C. (2001). Superconductivity in Dense ${\mathrm{MgB}}_{2}$ Wires. *Physical Review Letters*, *86*(11), 2423–2426. https://doi.org/10.1103/PhysRevLett.86.2423

Chen, P., Trociewitz, U. P., Davis, D. S., Bosque, E. S., Hilton, D. K., Kim, Y., Abraimov, D. V., Starch, W. L., Jiang, J., Hellstrom, E. E., & Larbalestier, D. C. (2017). Development of a persistent superconducting joint between Bi-2212/Ag-alloy multifilamentary round wires. *Superconductor Science and Technology*, *30*(2). https://doi.org/10.1088/1361-6668/30/2/025020

Chen, S. K., Majoros, M., MacManus-Driscoll, J. L., & Glowacki, B. A. (2005). In situ and ex situ Cu doping of MgB2. *Physica C: Superconductivity and Its Applications*, *418*(3–4), 99–106. https://doi.org/10.1016/j.physc.2004.11.011

Choi, J., & Lee, C. K. (2022). Development of a 1.2 MW Superconducting Induction Heater Using MgB2NI Magnets. *IEEE Transactions on Applied Superconductivity*, *32*(6). https://doi.org/10.1109/TASC.2022.3167649

Collings, E. W., Lee, E., Sumption, M. D., & Tomsic, M. (2002). Transport and magnetic properties of continuously processed MgB_2. *RARE METAL MATERIALS AND ENGINEERING*, *31*(6), 406–409.

Drung, D., Aßmann, C., Beyer, J., Kirste, A., Peters, M., Ruede, F., & Schurig, T. (2007). Highly sensitive and easy-to-use SQUID sensors. *IEEE Transactions on Applied Superconductivity*, *17*(2), 699–704. https://doi.org/10.1109/TASC.2007.897403

Egilmez, M., Ozyuzer, L., Tanoglu, M., Okur, S., Kamer, O., & Oner, Y. (2006). Electrical and mechanical properties of superconducting MgB2/Mg metal matrix composites. *Superconductor Science and Technology*, *19*(4), 359–364. https://doi.org/10.1088/0953-2048/19/4/019

Flükiger, R. L., Hossain, M. S. A., Kulich, M., & Senatore, C. (2012). Technical aspects of Cold High Pressure Densification (CHPD) on long lengths of in situ MgB2 wires with enhanced Jc values. *AIP Conference Proceedings*, *1435*, 353–362. https://doi.org/10.1063/1.4712116

Gajda, D., Morawski, A., Zaleski, A. J., Akdoğan, M., Yetiş, H., Karaboğa, F., Cetner, T., & Belenli, I. (2016). The influence of HIP process on critical parameters of MgB2/Fe wires with big boron grains and without barriers. *Journal of Alloys and Compounds*, *687*, 616–622. https://doi.org/10.1016/j.jallcom.2016.06.095

Giunchi, G., Ceresara, S., Ripamonti, G., Di Zenobio, A., Rossi, S., Chiarelli, S., Spadoni, M., Wesche, R., & Bruzzone, P. L. (2003). High performance new MgB_2 superconducting hollow wires. *SUPERCONDUCTOR SCIENCE & TECHNOLOGY*, *16*(2), 285–291. https://doi.org/10.1088/0953-2048/16/2/328

Guven, M., Zagura, P., Barker, C. M., Kutukcu, M. N., Atamert, S., Grovenor, C. R. M., & Speller, S. C. (2024). Persistent MgB2 joints for react and wind magnets. *Superconductor Science and Technology*, *37*(1). https://doi.org/10.1088/1361-6668/ad06c3

Hao, L., Macfarlane, J. C., Lam, S. K. H., Foley, C. P., Josephs-Franks, P., & Gallop, J. C. (2005). Inductive sensor based on nano-scale SQUIDs. *IEEE Transactions on Applied Superconductivity*, *15*(2 PART I), 514–517. https://doi.org/10.1109/TASC.2005.849892

Kalsi, S. S. (2014). Superconducting Wind Turbine Generator Employing MgB2 Windings Both on Rotor and Stator. *IEEE Transactions on Applied Superconductivity*, *24*(1). https://doi.org/10.1109/TASC.2013.2291275

Karaboğa, F., Yetiş, H., Akdoğan, M., & Belenli, İ. (2018). Monofilamentary In Situ Fe/MgB2 Superconducting Wires Fabricated by Pellet-in-Tube Method. *Journal of Superconductivity and Novel Magnetism*, *31*(5), 1359–1367. https://doi.org/10.1007/s10948-017-4335-7

Kodama, M., Tanaka, K., Okamoto, K., Yamamoto, A., & Shimoyama, J. I. (2019). Effect of the premixing of MgB2 powder on microstructures and electromagnetic properties in PIT-processed MgB2 wires. *Materials Research Express*, *6*(2). https://doi.org/10.1088/2053-1591/aaeeb8

Kostyuk, V. V., Antyukhov, I. V., Blagov, E. V., Vysotsky, V. S., Katorgin, B. I., Nosov, A. A., Fetisov, S. S., & Firsov, V. P. (2012). Experimental hybrid power transmission line with liquid hydrogen and MgB 2-based superconducting cable. *Technical Physics Letters*, *38*(3), 279–282. https://doi.org/10.1134/S106378501203025X

Kováč, P., Kopera, L., Kováč, J., Hain, M., Melišek, T., Kulich, M., & Hušek, I. (2018). Rutherford cable made of internal magnesium diffusion MgB2 wires sheathed with Al-Al2O3 particulate metal matrix composite. *Superconductor Science and Technology*, *31*(1). https://doi.org/10.1088/1361-6668/aa9539

Kwon, J., Rochester, J., Wan, F., Rindfleisch, M. A., Tomsic, M. J., Sumption, M. D., & Collings, E. W. (2023). Critical Current Densities and n-Values of MgB_2 Conductors for SMES, MRI, and Low AC Loss Applications. *IEEE Transactions on Applied Superconductivity*. https://doi.org/10.1109/TASC.2023.3247375

Ma, L., Suo, H. L., Zhang, Z. L., Gao, T. Y., Liu, M., Zhao, Y., Zhou, M. L., & Flükiger, R. (2008). Preparation of SiC doped In-Situ MgB2 mono- and 7-filamentary wires by continuous tube forming and filling technique. *Journal of Physics: Conference Series*, *97*(1). https://doi.org/10.1088/1742-6596/97/1/012242

Magnusson, N., Eliassen, J. C., Abrahamsen, A. B., Helleso, S. M., Runde, M., Nysveen, A., Moslatt, L. E., Bjerkli, J., & King, P. (2018). Fabrication of a Scaled MgB2 Racetrack Demonstrator Pole for a 10-MW Direct-Drive Wind Turbine Generator. *IEEE Transactions on Applied Superconductivity*, *28*(4). https://doi.org/10.1109/TASC.2018.2815027

Magnusson, N., Hellesø, S. M., Mikkonen, R., Abrahamsen, A. B., Runde, M., Berg, G., & Nysveen, A. (2021). Testing of an MgB2 coil for a wind turbine generator pole. *Physica C: Superconductivity and Its Applications*, *587*. https://doi.org/10.1016/j.physc.2021.1353901

Matsumoto, A., Hatakeyama, H., Kitaguchi, H., Togano, K., & Kumakura, H. (2003). The superconducting properties of MgB2/(stainless steel) tapes fabricated by the PIT process. *IEEE Transactions on Applied Superconductivity*, *13*(2 III), 3225–3228. https://doi.org/10.1109/TASC.2003.812206

Morandi, A., Fabbri, M., Ribani, P. L., Lo Franco, F., Mandrioli, R., Melaccio, U., Magrassi, D., Neri, M., Capelluto, A., Tropeano, M., & Gandolfi, C. (2023). Calculation of AC Losses in a 500 kJ/200 kW Multifilamentary MgB2 SMES Coil. *Energies*, *16*(4). https://doi.org/10.3390/en16041596

Morandi, A., Fiorillo, A., Pullano, S., & Ribani, P. L. (2017). Development of a Small Cryogen-Free MgB2 Test Coil for SMES Application. *IEEE Transactions on Applied Superconductivity*, *27*(4). https://doi.org/10.1109/TASC.2017.2653202

Mukoyama, S., Nakai, A., Sakamoto, H., Matsumoto, S., Nishijima, G., Hamada, M., Saito, K., & Miyoshi, Y. (2018). Superconducting joint of REBCO wires for MRI magnet. *Journal of Physics: Conference Series*, *1054*(1). https://doi.org/10.1088/1742-6596/1054/1/012038

Nagamatsu, J., Nakagawa, N., Muranaka, T., Zenitani, Y., & Akimitsu, J. (2001). Superconductivity at 39 K in magnesium diboride. *Nature*, *410*(6824), 63–64. https://doi.org/10.1038/35065039

Nagoshi, M., & Sato, K. (2014). SEM-EDS with low primary electron energy as a tool of surface analysis. *Surface and Interface Analysis*, *46*(10–11), 865–868. https://doi.org/10.1002/sia.5464

Norris, W. T., Power, A., & Willingham, ". (1997). Fault current limiters using superconductors. In *C~ogenics* (Vol. 37, Issue 97).

Patel, D., Al Hossain, M. S., Wai See, K., Xu, X., Barua, S., Ma, Z., Choi, S., Tomsic, M., & Ho Kim, J. (2015). MgB2 superconducting joints for persistent current operation. *Superconductor Science and Technology*, *28*(6). https://doi.org/10.1088/0953-2048/28/6/065017

Patel, D., Matsumoto, A., Kumakura, H., Hara, Y., Hara, T., Maeda, M., Liang, H., Yamauchi, Y., Choi, S., Kim, J. H., & Hossain, M. S. A. (2024). Superconducting joints using reacted multifilament MgB2 wires: A technology toward cryogen-free MRI magnets. *Journal of Magnesium and Alloys*, *12*(1), 159–170. https://doi.org/10.1016/j.jma.2023.11.014

Patel, D., Matsumoto, A., Kumakura, H., Maeda, M., Kim, S. H., Liang, H., Yamauchi, Y., Choi, S., Kim, J. H., & Hossain, M. S. A. (2021). Superconducting joints using multifilament MgB2 wires for MRI application. *Scripta Materialia*, *204*. https://doi.org/10.1016/j.scriptamat.2021.114156

Pei, X., Zeng, X., Smith, A. C., & Malkin, D. (2015). Resistive superconducting fault current limiter coil design using multistrand MgB2 wire. *IEEE Transactions on Applied Superconductivity*, *25*(3). https://doi.org/10.1109/TASC.2015.2390635

Ravindran, P., Vajeeston, P., Vidya, R., Kjekshus, A., & Fjellvåg, H. (2001). *Detailed electronic structure studies on superconducting MgB 2 and related compounds Typeset using REVT E X 2*.

Senatore, C., Al Hossain, M. S., & Flükiger, R. (2011). Enhanced connectivity and percolation in binary and doped in situ MgB 2 wires after cold high pressure densification. *IEEE Transactions on Applied Superconductivity*, *21*(3 PART 3), 2680–2685. https://doi.org/10.1109/TASC.2010.2096376

Suo, H. L., Ma, L., Jiang, J. M., Li, Y. M., Zhang, Z. L., Liu, M., Zhao, Y., He, D. Y., & Zhou, M. L. (2007). High critical current densities in SiC doped in-situ MgB2 wires prepared by continuous tube forming and filling technique. *IEEE Transactions on Applied Superconductivity*, *17*(2), 2822–2825. https://doi.org/10.1109/TASC.2007.897457